Cluster analysis and regression modelling of groundwater dynamics in Noord-Brabant: exploring key drivers for sustainable water management

Levi Yannick Biessen (VU Student Number: 2661598)

1st supervisor: prof. dr. Julia Schaumburg
2nd supervisor: dr. ir. Anne van Loon
3th supervisor: dr. ing. Jose David Henao Casas
co-reader: Matthijs ten Harkel

December 24, 2024

Abstract

This study addresses the increasing concern of groundwater sustainability by investigating the groundwater dynamics in the province of Noord-Brabant, a critical region for the drinking water supply of the Netherlands. Time series clustering and regression analyses are conducted to explore drivers of the fluctuations in groundwater. Clustering the SGI time series of multiple groundwater filters revealed patterns in the groundwater dynamics of distinct regions. Key findings include that short-to-medium-term meteorological dynamics, the SPEI_1 and SPEI_3, hold significant influence across all clusters. Specific clustered filters are characterized by elevated surface levels and the shallow depth of aquifers, whereas other clustered filters are identified for being positioned in deeply confined aquifers lying close to surface water bodies. The final regression models were able to explain a considerable fraction of the total variance in SGI. However, time-invariant numerical and categorical drivers such as elevation, proximity to surface water, water transition types and land use show negligible explanatory power. A critical research gap between local-scale and broad-scale analyses is filled as this research combines standardized hydrological indices with spatial clustering to derive actionable insights for targeted groundwater management.

Key words: Groundwater Dynamics, Cluster Analysis, Pooled Panel Regression, Meteorological Drivers, Hydrological Drought, Standardized Groundwater Index (SGI), Standardized Precipitation Evapotranspiration Index (SPEI), Noord-Brabant, Sustainable Water Management, Geological Formations, Spatial Variability, Multicollinearity, Land Use Patterns, Aquifer Recharge, Environmental Drivers.

Contents

1 Introduction

Water has always been a timeless subject in the Netherlands. Historically the main challenge was to deal with too much water and that's why the Netherlands is famous for its dikes. More recently however, the tables have turned: water scarcity has become a growing concern, specifically scarcity of groundwater. In the last 30 years, hydrological droughts have been dropping the groundwater levels, which causes major problems for our ecosystems, agriculture and urban areas. Groundwater, which provides over 50% of the world's urban population (Water et al., 2022), is especially important for the Netherlands. The Netherlands largely depends on Noord-Brabant, which is the country's main supplier of groundwater-based drinking water. The levels of these groundwater basins however, have been falling steadily in Noord-Brabant since the 1950s. The causes for this decline of groundwater include shifting land use, the rising human demand and climate change (Taylor et al., 2013; Cuthbert et al., 2019). In this study we dive into the causes behind this decline more deeply and aim to provide insights that can help manage groundwater sustainably in the future.

Even though hydrological drought is getting more and more attention nowadays, there's still a lot that we don't know about groundwater dynamics in Noord-Brabant. Especially when it comes to how groundwater dynamics differ per area and through time. Most studies focus on broad-scale factors like rainfall and evapotranspiration (Bloomfield et al., 2019), but factors like the type of geological formations, proximity to rivers or lakes, and land use patterns do not get as much attention. These factors are however also of great importance to understand how groundwater is replenished and how stable aquifers are. When considering how these local factors interact with larger climate trends, things get even more complicated. Without this knowledge, it's hard to develop targeted strategies for managing groundwater in specific areas.

This study takes on these challenges by looking at variations in groundwater levels across Noord-Brabant. **By grouping groundwater well filters based on their groundwater patterns over time, the study identifies the main drivers behind these fluctuations for different clusters**. The groundwater levels of the filters are firstly standardized into the Standardized Groundwater Index (SGI), to be able to compare filters correctly. The creation of filter groups with similar groundwater dynamics is done by the use of time series clustering techniques. Moreover, the Standardized Groundwater Index (SGI) and the Standardized Precipitation Evapotranspiration Index (SPEI) are computed for each filter individually, and hydrological and geological characteristics are connected to all filters. In this way, this study analyzes how weather, geology, and human activities shape the groundwater systems. By comparing spatial variability across clustered regions in Noord-Brabant, detailed insights to support sustainable groundwater management are offered compared to earlier research.

The results of this study indicate distinct regional patterns in the groundwater dynamics across Noord-Brabant, driven by both meteorological and categorical drivers. The regression analysis that was conducted shows that the first differences of SPEI_1 and SPEI_3, along with their lags, are the significant driver of fluctuations in ΔSGI in all clusters, with the lag of ΔSGI itself having a strong negative influence. In addition, categorical variables such as water transition types and, in one cluster, land use, are of importance

but do not provide considerable explanatory power. Furthermore, cluster *east_decr* has deep confined aquifers and relatively high elevations, whilst the cluster *central_east_decr* reveals intermediate filter depths and a high proportion of agricultural and forested land use at the surface level of the groundwater wells. The cluster *brabant_stat*, which contains spatially distributed filters across entire Noord-Brabant, yielded the highest adjusted R^2, indicating a successful representation of groundwater variability in the final regression model. On the other hand, clusters *west_decr* and *brabant_incr* are more affected by low-lying polders and big surface water interactions. These findings highlights the need to account for both short-term meteorological dynamics, as represented by SPEI, and local categorical drivers like geological formations, water transitions types, and land use, in designing targeted groundwater management strategies.

This study expands existing literature on groundwater by filling in the gaps between local-scale and larger-scale analyses. Spatial clustering techniques are combined with standardized hydrological indices in order to enable a new perspective into regional variability of groundwater. The study hereby gives insights to policy makers and water managers and aims to address the challenges posed by hydrological droughts in Noord-Brabant and similar regions in the Netherlands.

The rest of the thesis is organized as follows. Section 2 reviews relevant literature on the dynamics and management strategies of groundwater, focusing on the drivers of its variability. Section 3 describes the data that is used in this study and explains the methodological framework. In Section 4 the results are discussed by outlining the spatial patterns and the impact of specific drivers. Section 5 describes the implications of this research and provides potential future research. Finally, Section 6 concludes the main results.

2 Literature review

2.1 Groundwater

As groundwater is an essential component of fresh water on Earth, it plays a very important role in meeting the demand for human water consumption all over the world. In particular, approximately 50 percent of the global population is served by groundwater as primary source (Water et al., 2022). But what exactly is "groundwater"? The term groundwater can be defined as the water that is infiltrated into soil or subsoil originating either from surface water or precipitation. Since its infiltration, this water may remain stored underground for thousands of years (van Waterschappen, 2024; USGS, 2022). The water continues to seep into the soil until it reaches an impenetrable barrier, at which point the soil is completely saturated (USGS, 2022). This level at which the ground is completely saturated is referred to as the groundwater table and acts as the upper boundary where storage of groundwater begins, in so called aquifers. These aquifers are known to be sediment and rock formations that hold the groundwater reserves in the underground. Depending on the location, multiple aquifers can be found at different depths in the subsurface (Geographic, 2023).

Groundwater has numerous uses, including drinking water, agriculture, nature conservation, the production of energy and industry. It is therefore critical that the quantity and quality of groundwater remains preserved (van Waterschappen, 2024). Approximately two-thirds of the human population is directly or indirectly dependent on this groundwater to to meet all or most of their water needs (Gleeson et al., 2012). However, due to increased demographhic growth, most groundwater systems are under great pressure because of over-exploiting and contamination (Wada et al., 2010). This may lead to a number of environmental problems, including loss of groundwater storage, decline in water quality, and in extreme cases disappearance of ecosystems (Ferguson and Gleeson, 2012). Other issues in coastal locations include land subsidence and seawater intrusion (Jousma and Roelofsen, 2004; Ferguson and Gleeson, 2012).

2.2 Groundwater management

It is clear that a well-maintained groundwater balance is essential. Very high levels lead to flooding, while very low levels of groundwater may cause soil depletion, foundation damage, agricultural losses, and the drying out of sensitive flora (van Waterschappen, 2024; Alley et al., 2002). Therefore, it is very important to manage groundwater sustainably. Groundwater can only be managed effectively when there is proper knowledge of all the processes influencing its availability and quality (Sector, 2022).

In the Netherlands, provincial authorities provide strategic frameworks for groundwater management, while regional water authorities (waterschappen) are responsible for maintaining a healthy groundwater balance within regional water systems. This involves coordinating surface and subsurface activities within the groundwater system to mitigate depletion and flooding (van Waterschappen, 2024; of the Netherlands, 2022). The fact that more than half (55%) of the drinking water in the Netherlands comes from from groundwater further emphasizes the importance of this resource (Sector, 2022). Drinking water companies prefer groundwater because it is naturally filtered through layers of sand

and clay over long periods. These layers remove the contaminants and pathogens partially and therefore make the purification easier (van Waterschappen, 2024).

As a result, maintaining high-quality, fresh groundwater is very important to ensure the sustainability of drinking water supplies, agricultural productivity, and ecosystem health. As the demand on groundwater resources continues to grow, robust monitoring systems are vital to track the health and quality of these resources. Such monitoring systems support global efforts toward sustainable groundwater management and climate adaptation (Jousma and Roelofsen, 2004; Sector, 2022; van den Berg et al., 2019; RIVM, 2018). It is not sufficient to only monitor groundwater quality; we also have to know how the water levels fluctuate. Observing these fluctuations, which are captured by measuring the groundwater level, provides insights into the pressures and movements within the aquifers. However, if aquifers are poorly managed they risk depletion that can last centuries or more, through which water security for future generations can be threatened (of the Netherlands, 2022).

To address these challenges, various groundwater-focused management systems have been developed and implemented globally. These management systems try to maintain the balance between the competing forces of recharge and discharge while ensuring the sustainability of this critical resource. For example, the binary control-based management for groundwater extraction and recharge has been applied dynamically with real-time measurements of groundwater levels in Tianjin, China (Li et al., 2013). A number of other regions, particularly those with high levels of water stress, have adopted similar real-time monitoring systems to regulate extraction within defined thresholds (Sutanudjaja et al., 2021). The system works with two defined thresholds: firstly the blue line levels, which describe the long term sustainable levels necessary to protect the ecological and geological services that this groundwater is providing. This is an important basis for preventing environmental damage and securing groundwater resources (Lewandowski et al., 2020). The red line levels, on the other hand, describe the threshold beyond which significant and permanent environmental damage will be caused, such as land subsidence or saltwater intrusion (Li et al., 2013).

Given the unique hydrological conditions in the Netherlands, where large areas are situated below sea level, groundwater management systems are crucial here as well. Variations in groundwater levels have a direct impact on both the amount of water that is available and, less obviously, on land stability, as investigated in several regions in the United States (Galloway and Burbey, 2011). When groundwater levels in Noord-Brabant are not kept at the appropriate levels, for example, land could subside, causing damage to ecosystems and infrastructure (Witte et al., 2019). Furthermore, excessive groundwater abstraction can lead to drier and weakened, formerly wetlands and other vulnerable ecosystems in addition to disturbing the natural flow to surface water (Paulissen et al., 2007; Witte et al., 2019).

In order to have an effective management system, it is not enough to only have strategic frameworks and proactive policies. It is essential to monitor groundwater levels in real time, as this enables the assessment of recharge rates, to identify imbalances and to monitor the long-term trends. When combining good management practices with monitoring, groundwater reserves can be saved from the challenges that are created by climate change, land use changes, and population growth.

2.3 Monitoring groundwater head

Groundwater levels are key indicators for evaluating the health and sustainability of aquifers. These levels are measured using the groundwater head, derived from the hydraulic head. The groundwater head reflects both the pressure head exerted by the weight of the groundwater within an aquifer, and the potential head, which is related to the elevation of the groundwater level relative to a reference point. Together, these components represent the potential energy available to drive groundwater flow (Sector, 2022; Reitmeyer and colleagues, 2013). This pressure, which would be more accurately described as the potential energy per unit weight of groundwater, is of great importance in understanding the dynamics of groundwater. The head influences the water movement, as groundwater naturally moves from areas with a higher head to areas with a lower head. By this, the pressure in fact controls the distribution within the subsurface (Gleeson et al., 2015; Taylor and Alley, 2013).

To accurately measure groundwater heads at various depths in different aquifers, it is important to mention the differences between aquifer types. Aquifers are generally classified into two types: unconfined (phreatic) and confined. The phreatic aquifers are directly connected to the atmosphere, allowing groundwater head levels to respond dynamically to recharge events like precipitation (Gohari et al., 2023). Confined aquifers are more isolated from the direct surface interaction, by an impermeable layer. This layer restricts the aquifer to be immediately recharged and maintains groundwater under greater pressure (Li et al., 2024). As a result, phreatic aquifers show higher variability in groundwater head levels and often fluctuate with the seasonal changes in rainfall and evaporation Gohari et al. (2023). Groundwater levels in confined aquifers, however, are higher and more stable as they are less likely affected on the short-term (Li et al., 2024). Monitoring the differences in groundwater head variability across aquifers at different depths is therefore important in order to understand the recharge patterns and storage capacities in various aquifer types.

Groundwater head is generally measured as the height to which water rises in a well relative to a reference elevation, occasionally the mean sea level (Taylor and Alley, 2013). In the Netherlands, the reference elevation used is the NAP, or Normaal Amsterdams Peil (van Infrastructuur en Waterstaat, 2024; Peil, 2024). The groundwater head is ideally measured under static conditions; at the time when the head is measured, no water extractions are done in the area (Taylor and Alley, 2013). However, with automated recording devices, measurements may still be recorded during nearby water extractions. The validation process can then exclude these 'faulty' measurements to maintain the data quality. By examining the changes in groundwater head throughout time and space, hydrologists can derive important information on how the rates of recharge and discharge are balanced in an aquifer. For example, a drop in groundwater head might indicate that the discharge rate, whether through pumping or natural outflow, exceeds the recharge rate from rainfall or infiltration (Taylor and Alley, 2013; Rijkswaterstaat, 2024).

In regions like the province of Noord-Brabant (referred to for the remainder of this report as Noord-Brabant), the hydrological subsurface relies heavily on interaction with surface water, precipitation and human activities carried out in that region, such as agriculture, irrigation and industrial use (van Waterschappen, 2024). Fluctuations in the head

level of the groundwater in this area can indicate whether places have a broken recharge-discharge balance (Taylor and Alley, 2013). Long periods of low groundwater head levels are often a sign of over-extraction, which may lead to negative consequences like land subsidence or depletion of main water resources (Lewandowski et al., 2020). It is especially problematic in areas with a high population density or in industrial agriculture, where there is always a high demand for groundwater (Paulissen et al., 2007).

Robust data collection and analysis are necessary to ensure proper groundwater head level management and monitoring. For instance, regular monitoring can identify early warning signs of the imbalance between groundwater recharge and discharge, allowing for proactive action to be taken (Jousma and Roelofsen, 2004; Taylor and Alley, 2013). Therefore, by connecting subsurface processes with surface level ecological consequences like land deformation, groundwater head can also be used as an adequate indicator for larger environmental implications (Taylor and Alley, 2013; Galloway and Burbey, 2011).

Groundwater head levels are a useful asset in the recharge and discharge patterns, but they do have their own natural drivers from the environment as well. One primary factor is that climate change has introduced new complexities to the balances within groundwater systems. Learning how these trends influence groundwater head levels is key to addressing current and future issues.

2.4 Trends and climate change

Groundwater head changes are of great importance when depicting the recharge and discharge balance within aquifers. Groundwater head, and thus the rates of recharge and discharge, not only tends to fluctuate in direct response to precipitation and evapotranspiration, but also to human activities, like agricultural practices and industrial extraction (Taylor et al., 2013). Extraction exceeds natural recharge in many regions where groundwater is heavily used for irrigation, leading to long-term declines in groundwater levels (Gleeson et al., 2012). Climate change has played a huge role in accelerating these dynamics by shifting rainfall patterns and increasing evapotranspiration, which has resulted in groundwater systems being more vulnerable nowadays (Cuthbert et al., 2019). Rising temperatures and shifting precipitation patterns have increased drought risks by disrupting historical aquifer recharge rates (Famiglietti, 2014).

Unlike the gradual changes caused by natural seasonal fluctuations or long-term reductions by overextraction, drought presents special difficulties for groundwater systems. Drought events typically cause abrupt and temporary drops in groundwater levels since there is limited recharge and an increase in evaporation. Rising frequencies and intensity of drought is a clear example of anthropogenic warming, as mentioned by Bloomfield et al. (2019). For example, the droughts in Europe in 2018-2019 highlight continuing effects of declines in precipitation, increasing groundwater shortage over large areas (Brauns et al., 2020a). Groundwater drought can spread spatially and temporally through mechanisms like pooling and lagging, by which the impact of the drought is magnified and poses significant challenges to monitor and develop regional management strategies (Marchant et al., 2022; Bloomfield and Marchant, 2013). Even more important, aquifers like the chalk in the UK for example have a particularly high likelihood of being affected more severely by extended periods of drought because of their low recharge rates and storage properties (As-

cott et al., 2021). This shows the importance of distinguishing 'normal' fluctuations from the more acute and unpredictable effects of drought (Brauns et al., 2020b). This distinction is important to address known research gaps around groundwater drought behaviour and develop adaptive management strategies.

An Australian study has found that dry lands have a higher risk of structural groundwater head changes due to climate change. This is particularly severe in semi-arid and arid regions, where small variations in precipitation lead to significant groundwater level changes because of the low recharge rates (Taylor et al., 2013). On the other hand, the wetter regions showed to be more resistant. In a 26-year study in Queensland, Australia, agricultural areas were found to have groundwater levels dropping by an average of 0.06 m yearly, as these areas could not fully recharge the water that was lost during drought periods, even in wet seasons (Le Brocque et al., 2018). Groundwater levels in these agricultural areas were especially vulnerable to extended droughts, magnifying the effects of climate change on rainfall patterns and evapotranspiration (Fan et al., 2023). This trend emphasizes the increasing vulnerability of groundwater resources to long-lasting droughts, which is amplified by climate change and worsened by human extraction pressures (Famiglietti, 2014).

Semi-arid regions in India have experienced long-term groundwater head changes as a result of intensive agricultural groundwater extractions. 70% of irrigation relies on groundwater in the Indo-Gangetic Plains and this has caused that groundwater levels are now projected to fall with 12 meters by 2050 if current extraction rates continue. This depletion puts the Indian agricultural sustainability and energy consumption on the line, because more and more resources are required to pump water from the deeper subsurface (Patle et al., 2015).

The connection between groundwater and climate change is becoming clearer globally: according to a study on climate-groundwater interactions, locations where groundwater is heavily recharged by precipitation strongly are the most vulnerable to weather changes. Groundwater systems in arid locations adapt slowly to climate change, resulting in a temporal lag that hides the impact of reduced rainfall over decades (Cuthbert et al., 2019). This might delay the evident impacts of groundwater depletion, making proactive management more challenging. However, proactive management and prompt interventions are necessary.

In the Netherlands, especially in Noord-Brabant, groundwater is a very important resource for drinking water and agriculture. Groundwater head levels in Noord-Brabant have fallen between 0.2 and 0.3 meters since the 1950s (Witte et al., 2019). This drop is largely a result of altered land use (e.g. from grasslands to cities, and cropping practices), which has resulted in increased crop evapotranspiration and decreased natural recharge rates in the aquifers. The groundwater systems have been overburdened due to those challenges which pose a threat on much of Noord-Brabant's water demands (Witte et al., 2019).

Several intense droughts that started in 2018 worsened the situation in Noord-Brabant. The demands for irrigation and reduced rainfall, along with subsidence conditions, caused even bigger drops in groundwater head levels. The province faced significant water scarcity, further increasing pressure on groundwater supplies meant for both agricultural and urban needs. Industrial groundwater extraction, particularly brown coal mining in Germany for

instance, has also contributed to this decline. This resulted in making the long-term viability of the region's groundwater reserves uncertain (Brakenhoff et al., 2022; Witte et al., 2019).

In short: managing groundwater heads becomes increasingly difficult worldwide, including smaller regions like Noord-Brabant. Human activity and climate change place immense pressure on the groundwater resources of these areas. These combined pressures highlight the need to better understand groundwater fluctuations. Since these drivers directly affect groundwater head, it is important to understand them to effectively manage groundwater dynamics and prevent over-exploitation, especially in regions that are vulnerable to both environmental and human-induced changes.

2.5 Drivers of Groundwater Head

Precipitation is one of the most significant natural drivers recharging groundwater (Descroix et al., 2018), replenish aquifers and thus maintaining the level of groundwater in storage. This, however, has resulted in significant variations in the annual groundwater head levels as a result of changing precipitation patterns with climate change. A study in Germany, (Lewandowski et al., 2009), discovered that regions experiencing more consistent rainfall have less varying groundwater levels. Areas experiencing more irregular annual precipitation however, showed significant fluctuations in groundwater levels due to decreased recharge rates. A study in China showed that prolonged periods of reduced rainfall reduction, resulting from global warming, increased the severity of droughts and decreased groundwater recharge (Ren et al., 2024).

Another natural factor that affects groundwater head level is evapotranspiration. The evaporation rates rise due to temperature increases, further depleting the quantity of water available for infiltration and aquifer recharge. Research of the UK's Chalk aquifer noted that despite little change in precipitation, greater evapotranspiration (caused by climate change) increased the periods without effective recharge, placing the groundwater supplies under stress (Bloomfield et al., 2019). Areas in China showed same results where higher temperatures showed increased rates of evapotranspiration and led to lower groundwater recharge rates (Ren et al., 2024). Furthermore, a study employing quantile regression in the Netherlands, by Rashedy (2024) found that temperature and evaporation significantly predict groundwater levels during extreme drought conditions.

An example of human activities that significantly affect the groundwater head fluctuations is the extraction of groundwater for agriculture, industry, and urban use. Over-extracting groundwater can cause the groundwater levels to drop in such amounts that permanent aquifer depletion develops in the long term. According to Ren et al. (2024), researchers found that groundwater drought in China is associated more with human practices like water extraction than with meteorological conditions. Moreover, in India's Indo-Gangetic Plains, the unsustainable water extraction for irrigation has caused groundwater levels to fall by as much as 12 meters, putting the regional water supplies at risk (Patle et al., 2015).

Being close to surface water bodies like rivers and lakes plays a substantial role in local groundwater recharge. Groundwater systems with nearby surface water sources have shown to be more stable as they are refilled by these sources. As an example, groundwater

wells in the Yinchuan region of China that are close to the Yellow river recover far more quickly from drought than isolated groundwater wells that are not close to surface waters (Ren et al., 2024).

The geological formations that hold groundwater also shape the groundwater head levels. Formations like sandstone and limestone aquifers, yield stable groundwater levels due to their high permeability, while less permeable formations, like siltstone, mudstone and claystone, exhibit significant fluctuations. The permeable formations allow for faster water transmission and storage, while unpermeable formations restrict water movement, slowing down the recharge rates (Lewandowski et al., 2009). This is investigated by groundwater researchers in Germany finding out how different subsurface geological formations influence the groundwater table (Lewandowski et al., 2009). These findings emphasize how the regional and local geological characteristics of specific formations either transmit and store water quickly, or do neither, affecting groundwater availability over time. Over the border, groundwater in the Netherlands is held in sandy and gravelly aquifers that possess high permeability and quick transmission rates. However, changes in land use, increased evaporation, and decreased natural recharge have stressed these systems and lead to lower groundwater levels (Owuor et al., 2016).

In a nutshell, a variety of natural and human influences affect the groundwater head. As would be expected, the main natural drivers are precipitation and evaporation, which have been amplified last decades due to climate change. Extracting groundwater for agriculture use and industry is the key variable driven by human influence. Furthermore, the geology around a groundwater well filter in the subsurface and the proximity of a well to surface water also influences how much and how quickly groundwater levels are replenished. To understand groundwater dynamics and develop sustainable management practices, it is of great importance to get an idea of the interaction of these diverse variables.

3 Methodology

3.1 Data

The analyses in this research will be done on a data set covering the groundwater head levels in Noord-Brabant, and multiple potential drivers of the groundwater levels. As the data is gathered from different sources, they will be discussed separately.

3.1.1 Groundwater head

The groundwater head data used in this study are time series from Noord-Brabant, covering the period between 1988 and 2024 (September 1st), aggregated and provided by the province of Noord-Brabant, who receives them from Koenders Instruments. They make sure that at least 98% of the data is delivered. Unrealistic observations are cross-validated by the drinking water company, called Brabant Water, to make sure that at least 95% of the data is accurate. All data points that remain unexplained after the validation are removed from the dataset.

The data initially consisted of monthly to semimonthly head observations before 2011 and daily to hourly observations available from 2011 onward. The data for the period after 2011 was resampled from hourly to daily mean groundwater head observations, because of computational capacity and computational time efficiency. A couple of initial criteria were set for the data selection: each well filter must have data for at least 50% of the days, spanning a minimum of 8 years within the 2011 to 2024 period. Additionally, each well had to have known location coordinates (Province of Noord Brabant, 2024). Outliers were detected with the inter quartile range method (Walfish, 2006), in which the range between the first quartile, Q1, and the third quartile, Q3, of the whole dataset is determined. This is the middle 50% of the data, defined as the Inter Quartile Range (IQR). Outliers were identified as data points lying beyond 1.5 times the IQR below Q1 or above Q3 and were finally left out of the dataset. All these criteria resulted in a total of 296 groundwater well stations, each containing multiple filters at varying depths in the subsurface, adding up to a total of 719 station filters.

Gaps were initially not accounted for, to preserve the raw data integrity of the dataset. However, when calculating the Standardized Groundwater Index (SGI) (Bloomfield and Marchant, 2013), which will be explained in section 3.2.3, gaps were addressed. Since SGI calculations require monthly and continuous time series, the data was resampled to mean monthly values after which it was linearly interpolated for gaps up to 6 months. Unfortunately, the time series of a majority of the filters contained gaps of more than six months between 2008 and 2011. To maximize the number of groundwater well filters included in this study while ensuring an adequate observation period, the analysis period between 2011 and 2024 was eventually selected. This period provided the longest duration with the highest number of usable filters, resulting in 527 filters ultimately. See figure 1 on next page for the distribution of all filters in Noord-Brabant.

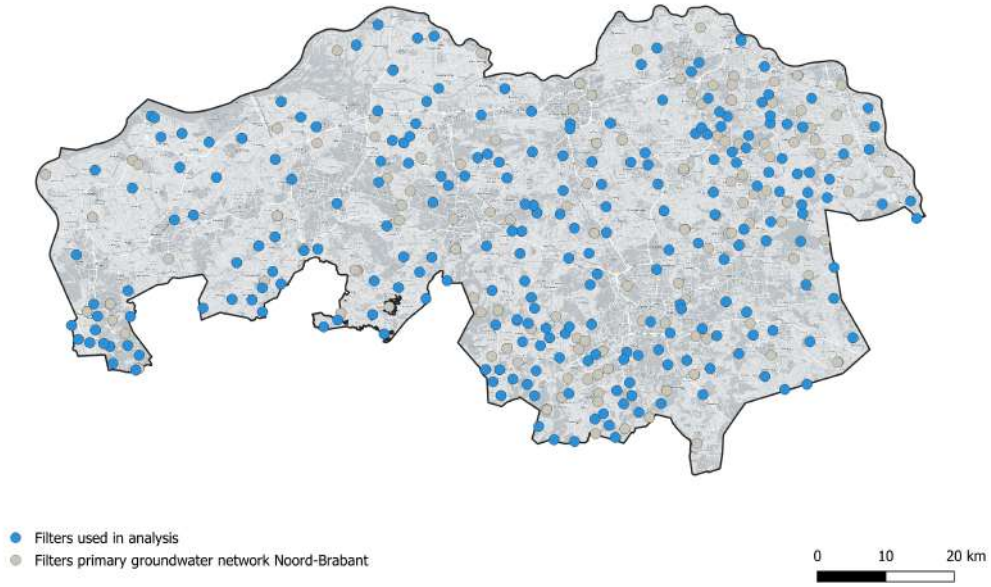

Figure 1: Spatial distribution of groundwater well filters in Noord-Brabant included in this study

3.1.2 Meteorological data

In this study, the impact of meteorological variability to groundwater levels will be evaluated by considering temperature, precipitation and evaporation. The data for each of these independent variables is acquired from the Koninklijk Nederlands Meteorologisch Instituut (KNMI), an institute that operates a national network of automatic weather and precipitation stations in the Netherlands(Koninklijk Nederlands Meteorologisch Instituut (KNMI), 2023).

The average daily temperature, which is recorded in 0.1 °C increments, follows clear seasonal patterns. In the summer the average temperature is higher and in the winter the average temperature is lower, with peaks around July-August and lows in January-February, a characteristic of the climate in the Netherlands (Koninklijk Nederlands Meteorologisch Instituut (KNMI), 2023).

Precipitation, which is measured as daily cumulative rainfall in 0.1 mm increments, does not show such clear seasonal cycles. Generally, there is more precipitation in winters than in summers, but with less intense rain showers, which increases the infiltration into the soil. This therefore contributes to seasonal variations in groundwater recharge as well. The pattern highlights the role of winter rainfall in replenishing groundwater reserves. Higher rainfall during the winter months, together with lower evaporation rates allows for more effective recharge (de Vries et al., 2020).

Evaporation, recorded in 0.1 °C mm increments, is a significant component in the Dutch (ground)water cycle, as mentioned before. A study by Hiemstra and Sluiter has shown that roughly 70% of the fallen precipitation is lost through evapotranspiration, which includes soil evaporation and transpiration from plants(Hiemstra and Sluiter, 2011). The Koninklijk Nederlands Meteorologisch Instituut (KNMI) (2023) calculates the reference evapotranspiration according to the Makkink method, by making use of shortwave radi-

ation and the daily mean temperature (Hiemstra and Sluiter, 2011). The predictability in the seasonal cycle of temperature is useful in understanding the seasonality of evapotranspiration rates and how the groundwater recharge rates shift every season. Lower temperatures go hand in hand with lower evapotranspiration, which in return allow for higher recharge rates, whereas the highest temperatures reached in summer also lead to the highest evaporation rates and lowest groundwater recharge rates (Jasechko et al., 2014).

The predictability in the seasonal cycle of temperature is useful in understanding the seasonality of evapotranspiration rates and how the groundwater recharge rates shift every season. Lower temperatures go hand in hand with lower evapotranspiration, which in return allow for higher recharge rates.

Daily time series of the mentioned climate variables were extracted from KNMI's weather stations to create the meteorological data series. Using Python's geopy library, the geodesic function was used to calculate the distances between each groundwater well's coordinates and the coordinates of the weather stations. Since not all KNMI weather stations contained complete data for each year since 1990, and some weather stations only provide data for a selection of the climatic variables, a list of the ten nearest weather stations for each well was created. By this, the data gaps were addressed by filling in missing observations with data from the next closest station. This resulted in making use of 12 weather stations across Noord-Brabant and the surrounding provinces in this study, as can be seen in Figure 2.

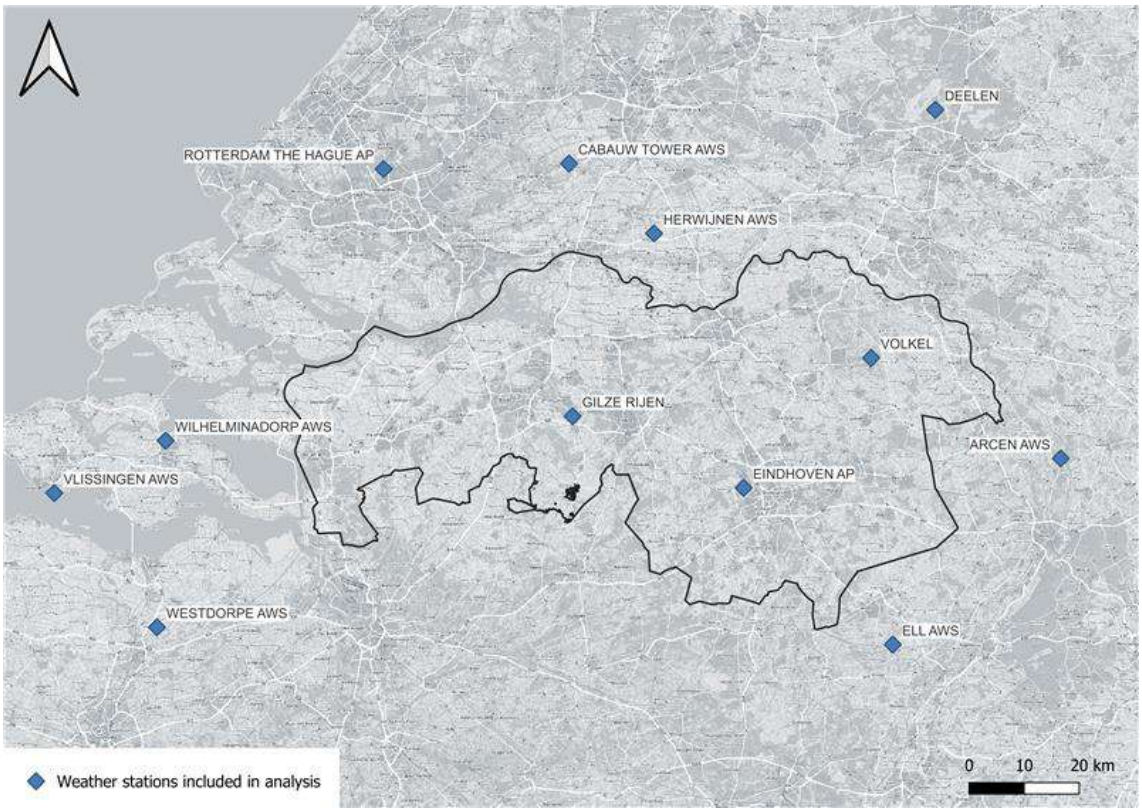

Figure 2: Spatial distribution of KNMI's weather stations in Noord-Brabant and surrounding provinces included in this study

3.1.3 Surface water bodies & water extraction wells

The precise coordinates of each groundwater well allow us to calculate their distance to the nearby surface water bodies. Using location data of the major rivers in Noord-Brabant (Geometrische begrenzing rivierbed grote rivieren) (Government of the Netherlands, 2019) and surface water bodies classified within KRW (Kader Richtlijn Water) (Nationaal Georegister, 2024) in GIS software, the minimum distance between each groundwater well and the surface water bodies was calculated. A distinction was initially made between larger rivers like the Maas and smaller KRW-designated water bodies. Since the Maas has such a large surface area and depth, it also influences groundwater recharge over a broad area in Noord-Brabant. This distinction is therefore important to understand its larger significance compared to other surface waters in the region. Additionally to the distance to surface water bodies, the water transition type of each groundwater well is of interest as well, as this better describes the waterland types around each well. The water transition types are categorized in beekdalen, flanken, hoge gronden, lokale laagtes, peelruggen, polders and uiterwaarden. The types were derived from HNS (Schengenga and Klijn, 2024), and were created in collaboration with Royal Haskoning.

Besides this, the known groundwater extraction wells in Noord-Brabant potentially having an impact on groundwater levels were included in this analysis. Using GIS software, the shortest distance from each groundwater well to the nearest water extraction location active after 2010 was determined. These distances help evaluate whether changes in groundwater heads show significant correlation with nearby extraction activities. Figure 3 illustrates the distribution of extraction locations that are active since 2010.

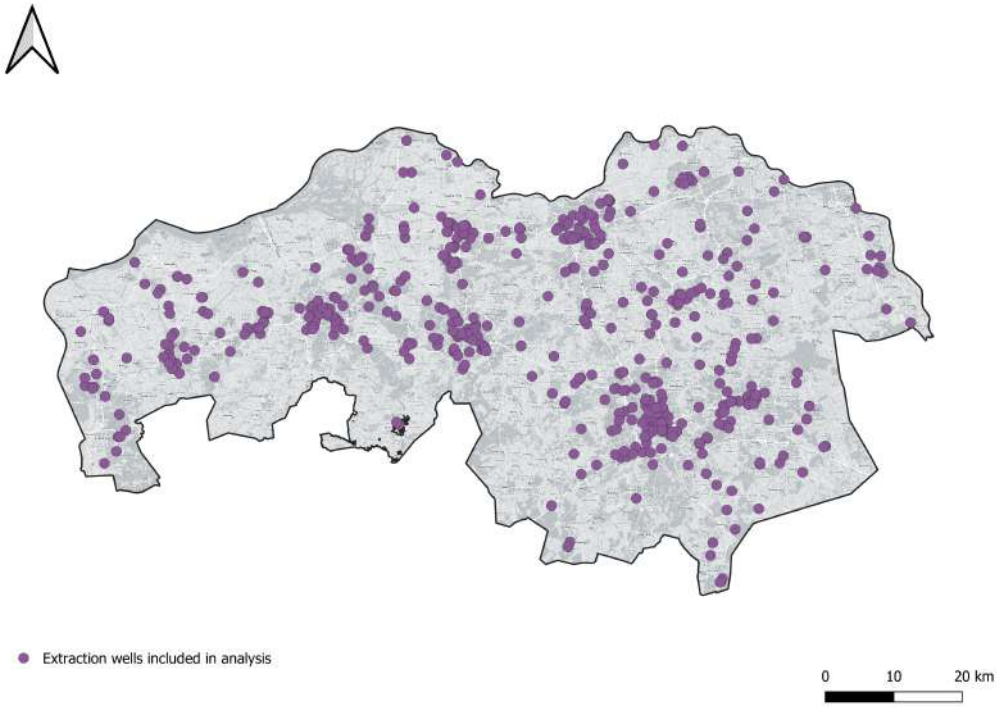

Figure 3: Spatial distribution of extraction locations in Noord-Brabant

3.1.4 Elevation, geological formation & land use

The groundwater well data provided by the Province of Noord-Brabant includes each well's surface level relative to the NAP standard. Thus, elevation data is available for each well and is considered in this study to evaluate its potential impact on groundwater head. The data shows elevation variation ranging from -1.4 to 42.7 meter. As the literature review suggested, elevation can potentially be an important factor influencing groundwater head.

The provincial data also provides filter depths (top and bottom) for each well. Since the subsurface of the Netherlands is well mapped in the REGIS-II model of the Dinoloket (Nederland, 2024), we can identify the geological formation associated with each well filter. The permeability of subsurface formations is a key property of the geological formations and affects groundwater flow and storage (European Environment Agency, 2024). Understanding the geological composition around each well thus supports a more accurate analysis of groundwater processes within the subsurface (of the province).

The land use data in this study is extracted from Landelijk Grondgebruik Nederland, LGN. They created a detailed land use map for the Netherlands, with the latest version updated in 2023 (Research, 2023). The LGN has been compiled by Wageningen Environmental Research based on satellite images and complemented with additional data sources and therefore reflects the latest actual land use situation of the Netherlands. The locations of the groundwater wells are linked with corresponding land use categories from the LGN map, by which 7 land use categories are assigned, including the agricultural areas, forests, water bodies, nature areas, remaining grass types, infrastructure and urban areas.

3.2 Standardization

When comparing multiple time series with differing scales of values - like the groundwater well filters where heads fluctuate around different means with different standard deviations - standardization is essential. By transforming the data to a common scale with a mean of zero and a standard deviation of one, it is possible to directly compare time series with the same variable, and even between time series of variables that are measured in different units (James et al., 2013). In this case we are talking about standardization based on the z-score, which involves subtracting the data by the mean and dividing by the standard deviation (Chow et al., 2021).

Before continuing, we should note that standardization requires a continuous time series with a sufficient sample size to ensure accuracy. Moreover, Z-score determination is based conceptually on the normal distribution (Chow et al., 2021). Hydrological variables, such as groundwater heads, precipitation, and evaporation, tend to show non-Gaussian distributions, and different groundwater well filters occasionally have distinct distributions (Wiemann and Katzfuss, 2023). This makes the general z-score standardization less applicable and that is why specific standardization approaches are created for the mentioned variables.

3.2.1 Standardized Precipitation Index

Precipitation is widely known to be standardized to the Standardized Precipitation Index (SPI). This index measures the precipitation surpluses and deficits that a certain area

experiences, based on the historical precipitation of that location. By this, the SPI quantifies meteorological drought. To quantify these droughts, ideally, monthly precipitation data with a continuous period of at least 30 years is used (McKee et al., 1993). First of all, a skewed probability distribution, occasionally the incomplete gamma distribution, is fitted to the raw monthly precipitation data to model the asymmetric variability. Afterwards, this fitted data is transformed into a normal distribution, enabling the calculation of dimensionless SPI values as z-scores:

$$\text{SPI} = \frac{P - P^*}{\sigma_p} \tag{1}$$

where P is the transformed precipitation, P^* is the mean transformed precipitation, and σ_p is it's standard deviation (Keyantash, 2021, 2023).

The SPI can be computed over different accumulation periods, with each period capturing different impacts of dry conditions: short intervals can detect immediate effects in falling or rising precipitation that effect soil moisture, while longer intervals detect long-term anomalies in precipitation that affect groundwater recharge amongst others. This versatility makes the SPI a widely used measure to analyse drought intensity and temporal dynamics of precipitation (Keyantash, 2021, 2023; McKee et al., 1993).

In this study we computed the SPI-1 and SPI-3, corresponding to one- and three-month accumulation computations, respectively. This decision was based on the short panel length of the groundwater data, spanning between 2011 to 2024. In general, shorter accumulation periods are more suitable for datasets with limited temporal scope, as they capture more immediate and granular meteorological effects (Insights, 2020). This approach ensures that the temporal variability and short-term drought dynamics are modeled adequately, considering the limitation in data. The SPI was computed using the standardized_precipitation_index function from the xclim.indices Python package (Bourgault et al., 2023, 2024).

3.2.2 Standardized Precipitation Evapotranspiration Index

By integrating the reference evapotranspiration (ET_0) into the SPI, the Standardized Precipitation Evapotranspiration Index (SPEI) is developed. This index accounts for both water availability and the potential evapotranspiration (PET). As the recharge (water balance) is calculated by precipitation minus evapotranspiration $P - ET_0$, the SPEI provides an improved measure of the drought severity. The SPEI namely captures temperature-driven changes in the evaporation and their influence on water stress (Vicente-Serrano, 2024; Vicente-Serrano et al., 2010).

The SPEI typically standardizes the recharge (P-ET) values using the log-logistic distribution, as this distribution is well-suited for skewed hydrological data. The resulting z-scores of this fitted data then make it possible to compare the recharge conditions of different regions across different periods. The same requirements regarding a continuous period of 30+ years are used as in the SPI calculations (McKee et al., 1993). Moreover, the SPEI is multi-scalar, like the SPI, which makes the index also applicable to evaluate drought impacts on short and long timescales. The inclusion of ET_0 and the multi-scalar capability give the SPEI the robustness and adaptability to link it with economic, agricultural, and hydrological effects of drought. This can provide valuable insights for policy

evaluation in water resource management (Vicente-Serrano, 2024; Vicente-Serrano et al., 2010).

The same decision regarding the one- and three month accumulation indexing was made for the SPEI. The SPEI is computed using the standardized_precipitation- _evapotranspiration_index function from the xclim.indices Python package (Bourgault et al., 2024).

3.2.3 Standardized Groundwater Index

The Standardized Groundwater Index (SGI) is a non-parametric index developed to quantify groundwater droughts by standardizing time series of groundwater heads. It builds on the principles of the SPI, but takes into account the more irregular patterns that are found in groundwater data (Bloomfield and Marchant, 2013).

Before computing the SGI values, monthly groundwater head levels were linearly interpolated for gaps up to 6 months, as mentioned in 3.1.1. All filters with data gaps larger than 6 months were left out in this analysis. This pre-processing guarantees accuracy and comparability of SGI calculations across diverse hydreological contexts. This resulted in 527 SGI time series for the period of 2012 until 2024 (13 years). This does conflict with the fact that McKee et al. (1993) suggested that data for a period of 30 years is required for SPI calculations. Since the SGI calculations are based on the SPI, the same requirements are expected for the SGI as can be seen in studies working with the SGI (Bloomfield and Marchant, 2013; Bloomfield et al., 2019; Wendt et al., 2020).

The SGI is computed by firstly ranking the historical groundwater head levels of each calendar month, for a given filter. These ranked values are then assigned equally spaced probabilities, after which the inverse normal cumulative distribution function is applied (Bloomfield and Marchant, 2013). This provides us with standard Gaussian values as SGI values, ranging from -1.769 to 1.769 in this study. Negative SGI values indicate dry conditions whereas positive values signify above-average groundwater levels. The SGI captures both seasonal variability and long-term trends, and therefore provides us with a non-parametric standardization approach that does not require fitting different distribution functions to each groundwater well filter. This makes the SGI a robust tool to assess groundwater anomalies and understand groundwater droughts across space and time (Wendt et al., 2020).

The SGI calculations in this study were computed by making use of the SGI function of the Python package called Pastas (Collenteur and Team, 2024). Groundwater drought is defined as a period of consecutive months with a SGI value smaller than -1 (Ebeling et al., 2024), based on the moderate SPI drought border ($<$ -1.0) categorized by McKee et al. (1993). With this definition, the number, average duration, and severity of drought events were calculated. The event severity was determined as the integral anomaly, based on cumulative SGI values during the event, as discussed by Ebeling et al. (2024). Lastly, monotonic trends in the SGI time series were analyzed using the Mann-Kendall trend test, with the original_test function from the Python package pyMannKendall (Hussain and Mahmud, 2019, 2024). It is important to note that for this test a minimum period of 30 years is required as well. As our analysis only covers 13 years, the definition of "trend" in this context should be interpreted as a statistically significant development signified within the period of 2012 until 2024, declared at a p-value threshold of 0.05.

3.3 Time series clustering

Time series clustering is the process of grouping data objects based on their temporal patterns into clusters in a way that maintains the sequential information of the data points (Aghabozorgi et al., 2015). This can particularly be of great value in hydrological datasets of groundwater well heads, where temporal time series properties of the data are critical in understanding the hydrological behaviour.

First of all, clustering is fundamentally based on calculating the pairwise distances between different objects. These objects are in our case the individual SGI time series of each filter. The clustering algorithm applied in this study is the k-means clustering algorithm, which is an unsupervised learning method that minimizes the within-cluster sum of squares (WCSS), which is the total sum of squared Euclidean distances between objects' data points within a cluster and the corresponding centroid in that cluster (Hartigan and Wong, 1979). It measures how well the objects are clustered, where a lower sum of squares describes a compact and better fit. The WCSS is calculated as follows:

$$W(C_k) = \sum_{x_i \in C_k} (x_i - \mu_k)^2 \tag{2}$$

where x_i is the ith data point of cluster k (C_k), and μ_k is the mean value of data points in cluster k (Ashani et al., 2022).

When translating the objects from the k-means clustering to time series objects, the Euclidean distance is used to quantify the similarities or dissimilarities between different time series. This Euclidean distance between time series can therefore be defined as follows:

$$D(r, s) = \sqrt{\sum_{t=1}^{T} (r_t - s_t)^2}, \tag{3}$$

where r and s are two time series, and r_t and s_t represent their respective t-th data points in time (Berthold and Höppner, 2016). Making use of this metric ensures that the clusters contain time series objects with minimal intra-cluster variability, thereby improving the homogeneity within each cluster.

Different clusters can have strong fits with the right objects in there, with a very low WCSS. However, minimizing the WCSS alone does not ensure that the different clusters are well separated. It is just as important to analyze whether clusters are overlapping or whether they stand alone compared to other clusters. In other words, the quality of clustering is accurately assessed by looking at the balance between the compactness of a cluster and the separation from other clusters. To address this balance, we employed two widely used validation techniques: the silhouette score and the elbow method.

The silhouette score evaluates both the compactness of clusters and their separation from one another and is computed as:

$$S = \frac{D_{\text{out}} - D_{\text{in}}}{\max(D_{\text{in}}, D_{\text{out}})}, \tag{4}$$

where D_{in} is the mean intra-cluster distance (the mean of how close object are to others within the same cluster), and D_{out} is the mean distance to the nearest neighboring cluster.

Scores range from -1, indicating poor or incorrect clustering, to 1, indicating well-separated and compact clustering, with 0 indicating overlapping clusters (Ashani et al., 2022).

The elbow method is another way of determining the optimal number of clusters, but then visually. By plotting the total WCSS against a range of cluster amounts, the optimal number of clusters can be identified at the "elbow point" on the curve. This is the point where the rate of decrease in WCSS significantly decreases (flattens out), and can be identified as the bend of an elbow. This is exactly the point that represents the balance between achieving compact clusters and avoiding overfitting by using too many clusters (Ashani et al., 2022).

We implemented the k-means algorithm using the KMeans function from the Python package called sklearn.cluster (Pedregosa et al., 2011). The k-means algorithm was applied to the SGI time series of the 527 groundwater well filters, where each time series becomes an object. 2 to 25 clusters were chosen to analyze in this study. First of all, we started with 25 initializations (n_init = 25) as starting points (centroids) for a cluster, and ran each initialization for 50 times (random states). Each initialization run was evaluated to determine the configuration with the best silhouette score. This led to potential cluster amounts of 2, 3 and 6. These cluster amounts were analyzed more robustly by running the K-means cluster with 500 initializations and 200 random states, which resulted in average distances ranging from 0.16 to 0.19. To make a better decision regarding the cluster, we made use of the Elbow method. Based on this method, we finally selected six clusters as the optimal number of clusters for our data set, with a silhouette score 0.16 and WCSS of 15577.5.

3.4 Unit root test

The presence of unit roots poses problems in statistical inference involving time series data. In particular, if a trend is present in the mean of a variable, this violates the stationarity condition, typically due to a unit root. In 2007 Pesaran proposed the unit root test, to test the null hypothesis H_0 that all panels contain a unit root, against the alternative hypothesis H_1 indicating that some panels are stationary.

In our analysis, however, we are more interested in testing whether all panels are stationary, rather than identifying the presence of unit roots in some panels. That is why we employ the Hadri unit root test (Hadri, 2000), which tests the null hypothesis H_0 that all panels are stationary, against the alternative hypothesis H_1 that at least one panel contains a unit root. The test statistic for the Hadri test is constructed using a residual-based Lagrange multiplier (LM), calculated from the residuals of the following regression model:

$$y_{it} = r_{i0} + \beta_i t + e_{it} \tag{5}$$

where y_{it} (for $t = 1, \ldots, T$ and $i = 1, \ldots, N$) represents the observed series being tested for stationarity for all panels i. Here, e_{it} are mutually independently and identically distributed (i.i.d.) normal errors across panels i and over time t, and r_0 are treated as fixed unknown parameters.

The test statistic is given by:

$$H_{LM,m} = \frac{1}{NT^2} \sum_{i=1}^{N} \sum_{t=1}^{T} \frac{S_{it}^2}{\hat{\sigma}_{ei}^2}, \quad \text{with} \quad \hat{\sigma}_{ei}^2 = \frac{1}{T} \sum_{t=1}^{T} \hat{e}_{it}^2 \tag{6}$$

The Hadri test assumes normality and requires a strongly balanced panel dataset (Hadri, 2000), making it suitable for analyzing this study's standardized variables $\text{SGI}_{i,t}$, $\text{SPI\_1}_{i,t}$, $\text{SPI\_3}_{i,t}$, $\text{SPEI\_1}_{i,t}$, $\text{SPEI\_3}_{i,t}$.

3.5 Correlation test SGI - SPI & SPEI

The correlation between the SGI, the SPI and the SPEI gives further insight into the relationship between dynamics of groundwater and meteorological drivers. It is important to analyze these correlations because SGI reflects changes in subsurface water storage, whereas SPI and SPEI capture the conditions of the atmosphere. Moreover, investigating the mentioned relationships helps detect the possible multicollinearity between the drivers, by which we can identify if one of the standardized indices is redundant for explaining the groundwater variability (Wheeler and Tiefelsdorf, 2005).

We evaluated the following correlation coefficients:

- $\Delta\text{SGI}_{i,t}$ with $\Delta\text{SPI\_1}_{i,t}$,$\Delta\text{SPI\_3}_{i,t}$, $\Delta\text{SPEI\_1}_{i,t}$, and $\Delta\text{SPEI\_3}_{i,t}$.
- $\Delta\text{SPI\_1}_{i,t}$ with $\Delta\text{SPI\_3}_{i,t}$, and $\Delta\text{SPEI\_1}_{i,t}$.
- $\Delta\text{SPEI\_1}_{i,t}$ with $\Delta\text{SPEI\_3}_{i,t}$.
- $\Delta\text{SPI\_3}_{i,t}$ with $\Delta\text{SPEI\_3}_{i,t}$.

These were computed using the pandas corrwith function in Python (Team, 2024a). In particular, the correlations are computed for each groundwater filter individually, after which the average is taken across all filters to get an overall measure, but also per cluster.

3.6 Multicollinearity test

Multicollinearity occurs when the independent variables in a regression model are highly correlated, resulting in the standard errors being inflated. This in return reduces the reliability of the estimates of the parameters, which indicates why multicollinearity is a problem (Wheeler and Tiefelsdorf, 2005). To diagnose this multicollinearity, the Variance Inflation Factor (VIF) is a widely used metric to calculate the severity of the multicollinearity in panel data models. The VIF determines how much the variance of the estimated regression coefficients are increased due to collinearity among drivers. It is calculated as follows:

$$\text{VIF}_j = \frac{1}{1 - R_j^2}, \tag{7}$$

where R_j^2 is the coefficient of determination when the j'th predictor is regressed on all other predictors in the model (Ismaeel et al., 2021). Calculated VIF values that are greater than or equal to 5, indicate that serious multicollinearity problems are present and that one of the analysed variables should be excluded or reduced in dimension. The VIF of the standardized meteorological indices was computed by using the variance_inflation_factor function from Python's statsmodels library (Team, 2024b)

3.7 Pooled panel regression analysis

Pooled panel regression is a statistical technique that combines cross-sectional data, from different filters with time series data into a single model. As it accounts for both spatial and temporal dimensions, this approach allows us to analyze the relationships between variables comprehensively, while accounting for variations over time and across filters. When analyzing the filters in separate cluster-specific cross-sectional models, the intra-cluster dynamics can be uncovered, and the inter-cluster dynamics can be explicitly compared. This explains the enhanced statistical power of the cluster-specific 'pooled' data.

To examine the relationships between the SGI and the environmental and spatial drivers, we will analyze the filters within each cluster separately, building the models from very simple to quite complex. In models 1A to 1D, we will analyze the SPI and SPEI firstly, with and without fixed effects, and make a decision on whether the added complexity of the evaporation component in SPEI is of such importance in explaining the SGI dynamics.

Fixed effects add a filter-specific constant α_i and time-specific effects α_t to the regression model. These constants hold all unobserved, time-(in)variant characteristics of each filter so that the estimated coefficients for the $\Delta\text{SPI\_}\cdot_{i,t}$ and $\Delta\text{SPEI\_}\cdot_{i,t}$ represent their true influence on SGI. The filter-specific fixed effects capture all the unobserved, time-invariant characteristics of each filter, like the geological and land use differences, and the time effects capture temporal variations common to all filters at the same time, like lagged influences, seasonal trends or region-wide climatic patterns. This ensures that estimated coefficients for SPI and SPEI are not biased and represent the actual impact on SGI.

In model 2 we will add the geological formations, water transitions types and land-use types, since these are expected to have most influence on the SGI, without interfering too much with each other, or other drivers. Next to the categorical variables, the lagged variable of SGI, $\Delta\text{SGI}_{i,t-1}$ is included. Finally, model 3A will include the lags of the meteorological variables, together with all time-invariant numerical variables. Ultimately, a final model is created with the most important drivers in model 3B.

3.7.1 Regression model 1

As explained, we will analyze the relationship between the Standardized Groundwater level Index (SGI) and its meteorological drivers separately for each cluster. This first form focuses on the influence of $\Delta\text{SPI\_}*_{i,t}$ without including fixed effects. The general form of model 1A is specified as follows:

$$\Delta\text{SGI}_{i,t} = \beta_0^{(k)} + \beta_1^{(k)}\Delta\text{SPI\_1}_{i,t} + \beta_2^{(k)}\Delta\text{SPI\_3}_{i,t} + \epsilon_{i,t}, \tag{8}$$

where i is the filter index, t is time, and k represents the cluster index. $\beta_0^{(k)}$ is the cluster-specific intercept, $\beta_1^{(k)}$ and $\beta_2^{(k)}$ are the regression coefficients for the meteorological drivers, $\Delta\text{SPI\_1}_{i,t}$ and $\Delta\text{SPI\_3}_{i,t}$, which are the first differences of SPI for 1-month and 3-month accumulation periods, respectively. Finally, $\epsilon_{i,t}$ represents the error term. This specification presents a simple cluster-specific regression model for investigating the short- and medium-term conditions of SPI on the dynamics of groundwater within each cluster.

When accounting for unobserved, time-invariant characteristics of individual filters and common time-specific effects, we employ the fixed effects regression model 1B. The general form of this model is specified as follows:

$$\Delta\text{SGI}_{i,t} = \beta_0^{(k)} + \beta_1^{(k)}\Delta\text{SPI\_1}_{i,t} + \beta_2^{(k)}\Delta\text{SPI\_3}_{i,t} + \alpha_i + \alpha_t + \epsilon_{i,t}, \tag{9}$$

where the same descriptions hold as for model 1A. The two terms that are added are α_i and α_t, the fixed effect for each filter i and the time-specific fixed effect. This ensures that the estimated coefficients for ΔSPI_1 and ΔSPI_3 represent their true influence on ΔSGI, independent of filter-specific and time-dependent factors.

In model 1C, the focus will be on the influence of $\Delta\text{SPEI\_*}_{i,t}$. The general form of this model, without including fixed effects, is specified as follows:

$$\Delta\text{SGI}_{i,t} = \beta_0^{(k)} + \beta_1^{(k)}\Delta\text{SPEI\_1}_{i,t} + \beta_2^{(k)}\Delta\text{SPEI\_3}_{i,t} + \epsilon_{i,t}, \tag{10}$$

where the same conditions hold as for model 1A, except for $\Delta\text{SPEI\_1}_{i,t}$ and $\Delta\text{SPEI\_3}_{i,t}$, which are the first differences of SPEI for 1-month and 3-month accumulation periods, respectively.

When accounting for unobserved characteristics of individual filters and common temporal variations, we employ fixed effects regression model 1D:

$$\Delta\text{SGI}_{i,t} = \beta_0^{(k)} + \beta_1^{(k)}\Delta\text{SPEI\_1}_{i,t} + \beta_2^{(k)}\Delta\text{SPEI\_3}_{i,t} + \alpha_i + \alpha_t + \epsilon_{i,t}, \tag{11}$$

where the same descriptions hold as for model 1C. The additional terms are α_i, the fixed effect for each filter i and α_t, which is the time-specific fixed effect.

3.7.2 Regression model 2

In Model 2, we extend the analysis by incorporating the first lag of ΔSGI, as well as the water transition type, geological formation and land-use type as categorical variables. These variables are expected to provide additional explanatory power by accounting for differences in geological and hydrological contexts across filters and adding historical lags to the model. Furthermore, the addition of $\Delta\text{SGI}_{i,t-1}$ captures persistence of past values. The model is specified as follows:

$$\begin{aligned}\Delta\text{SGI}_{i,t} = \beta_0^{(k)} + \beta_1^{(k)}\Delta\text{SGI}_{i,t-1} + \beta_2^{(k)}\Delta\text{SPEI\_1}_{i,t} + \beta_3^{(k)}\Delta\text{SPEI\_3}_{i,t} \\ + \sum_{j=1}^{J}\gamma_j W_{j,i} + \sum_{l=1}^{L}\delta_l G_{l,i} + \sum_{m=1}^{M}\eta_m L_{m,i} + \epsilon_{i,t},\end{aligned} \tag{12}$$

where i is the filter index, t is time, and k represents the cluster index. $\beta_0^{(k)}$ is the cluster-specific intercept, $\beta_1^{(k)}$, $\beta_2^{(k)}$ and $\beta_3^{(k)}$ are the regression coefficients for the first lag of ΔSGI and the meteorological drivers.[1] The terms $W_{j,i}$, $L_{m,i}$ and $G_{l,i}$ are added to this model and represent the water transition type, land use type at the surface level of the filter, and

[1]Notice that $\beta_1^{(k)}$ is now the coefficient of $\Delta\text{SGI}_{i,t-1}$, and $\beta_2^{(k)}$ and $\beta_3^{(k)}$ are coefficients of $\Delta\text{SPI\_1}_{i,t}$, and $\Delta\text{SPI\_3}_{i,t}$ respectively.

the geological formation surrounding the filter, respectively, with γ_j, δ_l and η_m as their regression coefficients, respectively. The optimal regression model is determined for each cluster, likely resulting in varying combinations of explanatory drivers across clusters.

3.7.3 Regression model 3

In Model 3, we extend the analysis by adding several time invariant numerical variables to model 2: elevation, filter depth, proximity to big surface water, proximity to KRW surface water, and the proximity to extraction locations. Furthermore, the lags of $\Delta\text{SPI\_1}_{i,t}$ and $\Delta\text{SPI\_3}_{i,t}$ are added to this model. These variables are expected to provide additional explanatory power by accounting for differences in location-related contexts across filters.

$$\begin{aligned}\Delta\text{SGI}_{i,t} = \beta_0^{(k)} + \beta_1^{(k)}\Delta\text{SGI}_{i,t-1} + \beta_2^{(k)}\Delta\text{SPEI\_1}_{i,t} + \beta_3^{(k)}\Delta\text{SPEI\_3}_{i,t} + \beta_4^{(k)}\Delta\text{SPEI\_1}_{i,t-1} \\ +\beta_5^{(k)}\Delta\text{SPEI\_3}_{i,t-1} + \sum_{j=1}^{J}\gamma_j W_{j,i} + \sum_{l=1}^{L}\delta_l G_{l,i} + \sum_{m=1}^{M}\eta_m L_{m,i} + \phi_1^{(k)}\text{elevation}_i \\ +\phi_2^{(k)}\text{Depth}_i + \phi_3^{(k)}\text{prox\_bigSW}_i + \phi_4^{(k)}\text{prox\_KRW}_i + \phi_5^{(k)}\text{prox\_extract}_i + \epsilon_{i,t},\end{aligned} \tag{13}$$

where i is the filter index, t is time, and k represents the cluster index. $\beta_0^{(k)}$ is the cluster-specific intercept, $\beta_1^{(k)}$, $\beta_2^{(k)}$, $\beta_3^{(k)}$, $\beta_4^{(k)}$ and $\beta_5^{(k)}$ are the regression coefficients for the first lag of ΔSGI, the meteorological drivers and their first lags. The terms γ_j, δ_l and η_m represent the regression coefficients of the water transition type, geological formation and land-use type respectively. And finally $\phi_1^{(k)}$ until $\phi_5^{(k)}$ are the regression coefficients for the time-invariant numerical variables in each cluster.

Firstly, the whole model including all variables is created for each cluster. To finalize model 3, a specific model with the most influential drivers of the ΔSGI is created for each cluster.

The regression models in this research were conducted by making use of Python packages linearmodels and statsmodels, of which the functions PanelOls and OLS were used, respectively (Sheppard, 2024; Seabold and Perktold, 2024). Since in model 1 entity and time fixed effects were included, the function PanelOls was chosen for its usability. From model 2 onwards, the emphasis was no longer on isolating within-filter or within-time effects, but understanding the aggregate influence of predictors across the cluster as a whole. This made the fixed effects functionality unnecessary for this part of the analysis, so we continued with the OLS function. This function treats the data as pooled and provides extra measures to assess the regression analysis, such as the adjusted r squared, AIC (Akaike infomation criterion) and the BIC (Bayesian infomation criterion).

The results are assessed using the R^2 and adjusted R^2, which measure the fraction of the total variance in ΔSGI that is explained by the model's drivers. The adjusted R^2 corrects for the loss of degrees of freedom resulting from the inclusion of extra regression variables. It therefore provides a more reliable measure of the model fit (Miles, 2005).

4 Results

In this section, we show the results obtained using the different methods explained in section 3. We begin by exploring the clusters that were created by the K-means algorithm in section 4.1 and describe their distinct characteristics. Following this, from section 4.2 onwards, we outline the results of the preparation analyses conducted for the regression models. These analyses include the Unit Root Hadri Test, Correlation Test, and Multicollinearity VIF Test. Finally, section 4.5 presents the findings of the regression analyses regarding the different models described in the methodology.

4.1 Variability in clusters

Overall, the SGI time series across the investigated groundwater well filters exhibited both temporal and spatial variability. Six clusters of SGI time series were identified, revealing distinct regional patterns in groundwater drought responses, which is shown in figure 4 on pages 27 and 28. Clusters *brabant_stat* and *brabant_incr* are spread across the entire Noord-Brabant, while cluster *brabantse_wal_decr* is clearly concentrated in three areas: one area is the Brabantse Wal (where a majority of the filters are located), another is centered along the Feldbissbreuk near the city of Tilburg and a minor area south-west of the city of Eindhoven. Clusters *east_decr* and *central_east_decr* are located more in the eastern part of Noord-Brabant, while cluster *west_decr* shows filters that are solely located in the western part of the province. The distribution among the clusters ranges from 39, in cluster *brabantse_wal_decr* (7.2%) to 201, in cluster *central_east_decr* (38.1%), with clusters *east_decr*, *brabant_stat*, *west_decr* and *brabant_incr* containing 54, 112, 79 and 42 filters, respectively.

Results of the Mann-Kendall trend test, which are presented in table 1 on page 29, reveal significant negative trends across the 14 years of monthly SGI's were observed in 44.6% of the filters and positive trends only in 12.7%. Across clusters, the number of positive and negative trends in SGI varied, with all filters in cluster *east_decr* having negative trends (100%) and cluster *brabant_incr* being dominated by positive trends (95.2% vs. 0% negative[2]) trends. Cluster *central_east_decr* and *west_decr* showed a balance between negative trends (50.2% and 49.4%, respectively) and no significant trend (48.8% and 50.6% , respectively)[3]. For cluster *brabantse_wal_decr*, 92.3% showed a decreasing trend, with an increasing trend and no trend for 2.6% and 5.1% of the filters, respectively. For cluster *brabant_stat* only 4.5% of the filters showed negative trends, 21.4% showed positive trends with a resulting 74.1% filters having no trend.

According to these observed characteristics, clusters were categorized in terms of regional prevalence (east, west, central_east, brabantse_wal, and brabant, with the last one representing clusters distributed across all of Noord-Brabant) and the dominant trend in SGI time series (incr - increasing trend, decr - decreasing trend, and stat - stationary trend). This resulted in the clusters *east_decr*, *brabantse_wal_decr*, *central_east_decr*, *brabant_stat*, *west_decr* and *brabant_incr*. The distribution of clustered filters and the average SGI time series for each cluster are presented in figure 4 on pages 27 and 28.

[2]The rest of the filters showed no significant trend

[3]The remaining 1.0% (2) of the filters in cluster *central_east_decr* had a positive trend

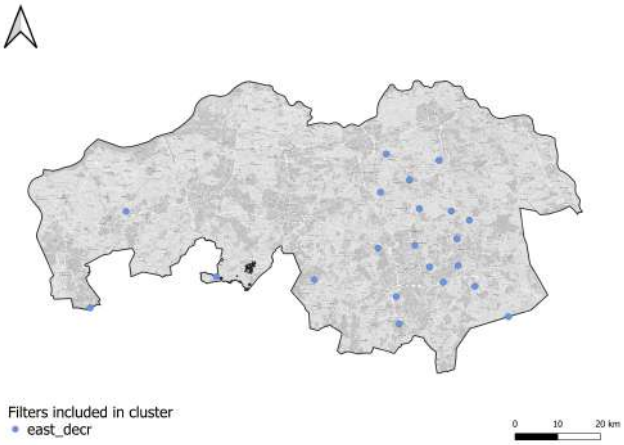

(a) Map of Noord-Brabant - *east_decr*

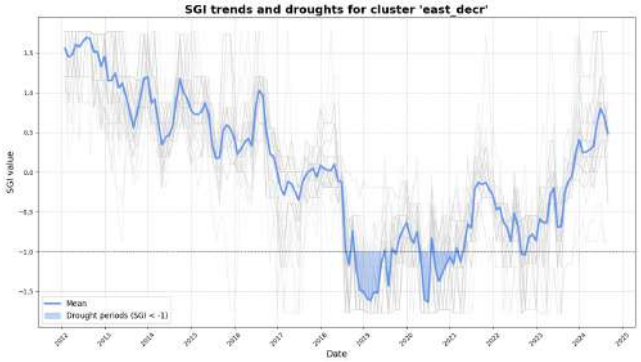

(b) SGI time series - *east_decr*

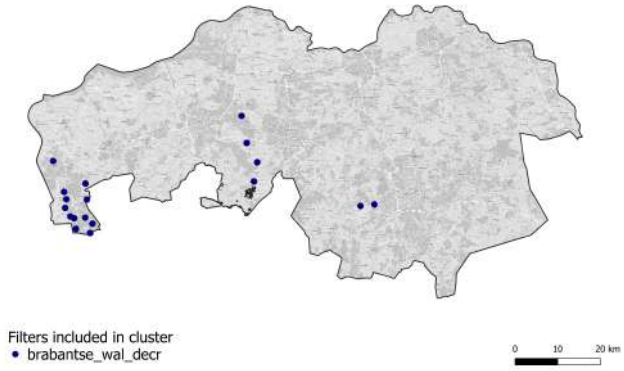

(c) Map of Noord-Brabant - *brabantse_wal_decr*

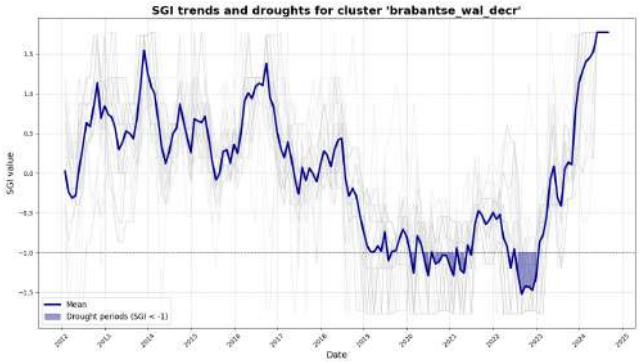

(d) SGI time series - *brabantse_wal_decr*

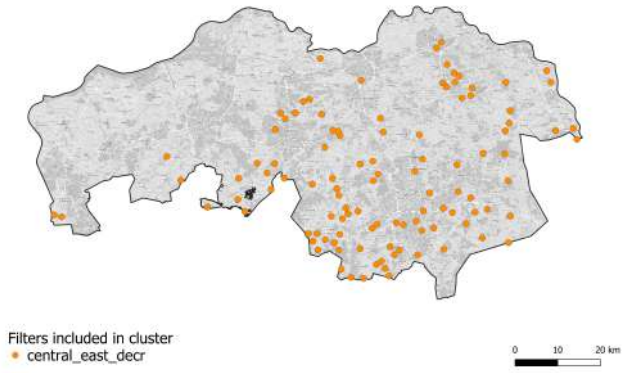

(e) Map of Noord-Brabant - *central_east_decr*

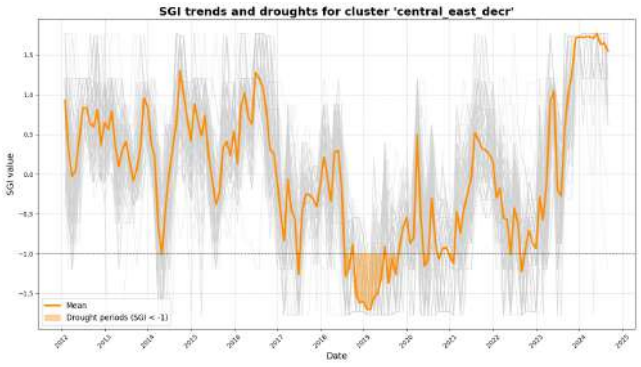

(f) SGI time series - *central_east_decr*

Figure 4: Cluster maps on the left and SGI time series on the right for clusters 1 to 3.

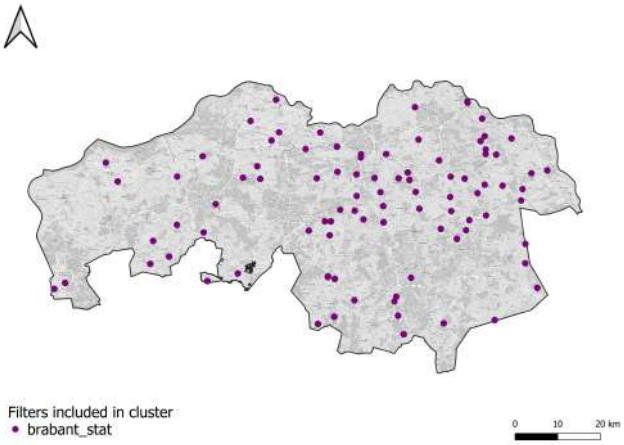

(g) Map of Noord-Brabant - *brabant_stat*

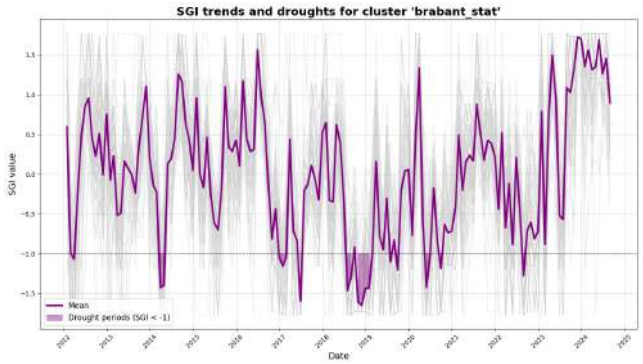

(h) SGI time series - *brabant_stat*

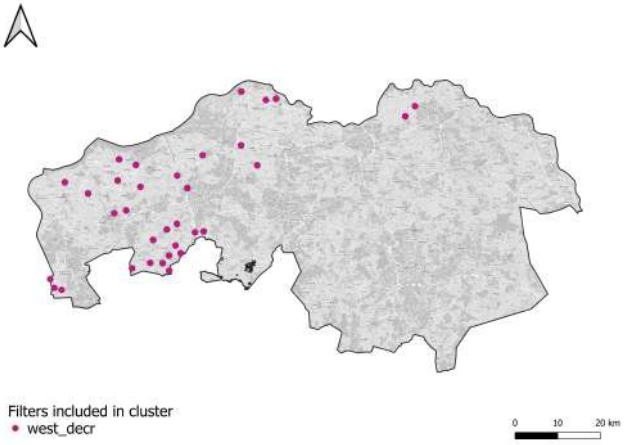

(i) Map of Noord-Brabant - *west_decr*

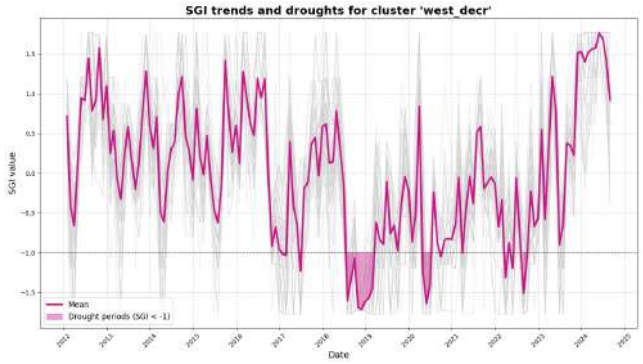

(j) SGI time series - *west_decr*

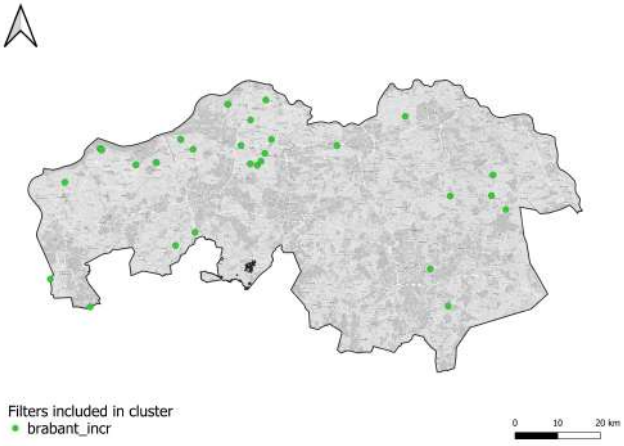

(k) Map of Noord-Brabant - *brabant_incr*

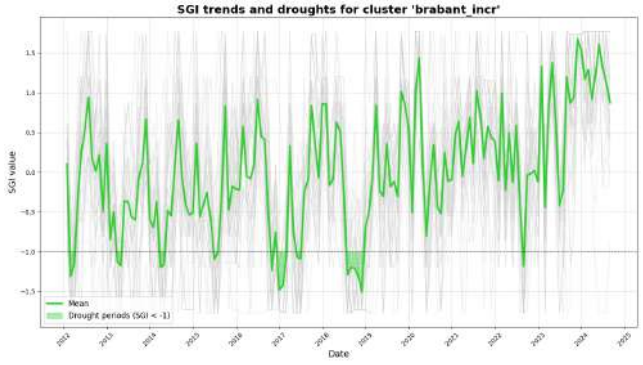

(l) SGI time series - *brabant_incr*

Figure 4: Cluster maps on the left and SGI time series on the right for clusters 4 to 6.

Drought duration is right-skewed across all clusters, with cluster *east_decr* having the longest droughts (an average of 6 months and 18 days) and cluster *brabant_stat* having the shortest (an average of 3 months and 6 days). Overall droughts lasted an average 4 months and 3 days. This resulted in the average drought severity ranging from -4.9 (cluster *brabant_stat*) to -9.8 (cluster *east_decr*), with an overall mean severity of -6.12. The amount of drought periods in each cluster ranged from 4.0 (cluster *east_decr* and *brabantse_wal_decr*) to 5.5 (clusters *brabant_stat*), with filters experiencing 4.7 drought periods overall.

Cluster	**Trend**	**Count**	**Percentage (%)**
east_decr	Decreasing	54	100.00
brabantse_wal_decr	Decreasing	36	92.31
	Increasing	1	2.56
	No trend	2	5.13
central_east_decr	Decreasing	101	50.25
	Increasing	2	1.00
	No trend	98	48.76
brabant_stat	Decreasing	5	4.46
	Increasing	24	21.43
	No trend	83	74.11
west_decr	Decreasing	39	49.37
	No trend	40	50.63
brabant_incr	Increasing	40	95.24
	No trend	2	4.76
Overall	**Decreasing**	**235**	**44.59**
	Increasing	**67**	**12.71**
	No trend	**225**	**42.69**

Table 1: Results of the Mann-Kendall trend test

Cluster	**Drought duration**		**Drought severity**		**Drought events**
	Mean	**Median**	**Mean**	**Median**	**Mean**
east_decr	6.6	4.5	-9.8	-6.3	4.0
brabantse_wal_decr	5.8	5.0	-8.6	-7.3	4.0
central_east_decr	5.1	3.0	-7.6	-4.7	4.2
brabant_stat	3.2	2.0	-4.9	-3.5	5.5
west_decr	3.9	3.0	-5.9	-4.7	5.0
brabant_incr	3.5	2.5	-5.3	-3.6	5.5
Overall	**4.1**	**3.0**	**-6.2**	**-4.0**	**4.7**

Table 2: Summary of drought characteristics by cluster

When zooming in on the means and medians of the different numerical drivers of SGI, whose influence will be analyzed in section 4.5, some interesting assumptions can be drawn. Find table 3 on page 31 for a full overview. First of all looking at the elevation, cluster *central_east_decr* showed the highest mean, of 20.34 meter, suggesting the filters are located in (slightly) elevated areas, which is typical for the central and eastern part of Noord-Brabant. In contrast, clusters *west_decr* and *brabant_incr* have the lowest elevations with means of 4.17 and 4.09, indicating they are in low-lying regions. Cluster *brabant_stat* shows moderate elevation but exhibits the greatest variability between its mean (12.33) and median (10.77), which can be assigned to this cluster being spread all over Brabant. These surface level characteristics suggest that clusters *central_east_decr* and *east_decr* are less influenced by surface water processes, while clusters *west_decr* and *brabant_incr* are more prone to surface water impacts due to their low elevations.

When analyzing the filter depths, cluster *east_decr* stands out with exceptionally deep filters with a mean of -182.43 m NAP, making it relatively isolated from surface-driven processes such as precipitation and evaporation. Clusters *brabantse_wal_decr* and *brabant_stat* have the shallowest filters, with cluster *brabant_stat* being the shallowest overall mean (-3.02 m NAP), indicating greater interaction with surface-driven processes. Clusters *central_east_decr*, *west_decr* and *brabant_incr* fall in the intermediate range, showing a balance between shallow and moderately deep filters.

Proximity to surface water highlights clear distinctions among clusters as well. Cluster *brabantse_wal_decr* is the most isolated from large surface water bodies like the Maas, with a mean of 30,077 meters. Clusters *east_decr* and *central_east_decr* are on average also quite isolated with 23,725 and 24,514 meters on average, respectively, while cluster *brabant_incr* is on average the closest (mean of 7,663 m and a median of = 2,267 m), followed by cluster *west_decr* (mean = 12,429 m, median = 11,050 m). This would suggest that clusters *brabant_incr* and *west_decr* are more affected by large surface water recharge, whereas clusters *east_decr*, *brabantse_wal_decr* and *central_east_decr* act more independently from surface water fluctuations. Regarding the smaller water bodies (KRW), there are no huge differences found between clusters. Cluster *brabantse_wal_decr* is the most distant with a mean of 2,168 meter whereas clusters *brabant_stat* and *west_decr* are the closest, at a distance of 400-500 meter. In a nutshell, clusters *brabant_stat*, *west_decr*, and *brabant_incr* show the strongest proximity and potential interaction with surface water, while cluster *brabantse_wal_decr* is most isolated.

Lastly the distance to extraction locations: cluster *brabant_incr* is on average the furthest away from the extraction locations, with a mean of 4,218 m, while cluster *east_decr* is the closest (mean of 2,042 m). These results indicate that cluster *east_decr* is likely to experience unique hydrological impacts due to its proximity to the extractions of groundwater.

Besides the numerical drivers, the categorical variables further explain heterogeneity across the clusters. All dominant geological formations at the subsurface depth where the filters are situated in are found to be sandy units. However, the grain size, permeability, porosity and stratification of these formations vary and influence groundwater dynamics differently. For example, the PZWAz formation (Peize and Waalre) dominates the formations of the filters in clusters *east_decr*, *brabantse_wal_decr*, *west_decr*, and *brabant_incr* and has relatively homogeneous conditions of groundwater recharge and storage, as it exhibits

Summary statistics of time-invariant variables per cluster												
	Cluster 1: *east_decr*		**Cluster 2: *brabantse_wal_decr***		**Cluster 3: *central_east_decr***		**Cluster 4: *brabant_stat***		**Cluster 5: *west_decr***		**Cluster 6: *brabant_incr***	
Vars.	Mean	Median	Mean	Median	Mean	Median	Mean	Median	Mean	Median	Mean	Median
Elevation	16	14	14	14	20	21	12	11	4	4	4	1
Filter depth	-182	-172	-14	-10	-31	-3	-3	1	-65	-53	-34	-10
Proximity to big SW	23,725	22,946	30,077	31,582	24,514	26,120	16,857	15,460	12,429	11,050	7,663	2,267
Proximity to KRW SW	976	754	2,168	1,384	764	605	517	398	446	405	774	508
Proximity to extraction location	2,042	1,341	3,054	2,488	3,282	2,678	2,776	2,381	3,943	3,395	4,218	4,196

Top 3 Geological formations, Land use types, and Water transition types per cluster						
	Cluster 1: *east_decr*	**Cluster 2: *brabantse_wal_decr***	**Cluster 3: *central_east_decr***	**Cluster 4: *brabant_stat***	**Cluster 5: *west_decr***	**Cluster 6: *brabant_incr***
Top 3 Geological formations	1. PZWAz (20) 2. KIz (17) 3. BRz (5)	1. PZWAz (18) 2. OOz (8) 3. STz (3)	1. STz (39) 2. PZWAz (35) 3. BXz (25)	1. BXz (36) 2. STz (24) 3. BEz (19)	1. PZWAz (25) 2. MSz (17) 3. OOz (13)	1. PZWAz (10) 2. KRz (7) 3. HLc (6)
Top 3 Land use types	1. Agrarisch gebied (20) 2. Bos (18) 3. Natuur (6)	1. Bos (11) 2. Bebouwd gebied (10) 3. Agrarisch gebied (9)	1. Bos (58) 2. Agrarisch gebied (56) 3. Infrastructuur (32)	1. Agrarisch gebied (35) 2. Bos (24) 3. Infrastructuur (19)	1. Agrarisch gebied (31) 2. Infrastructuur (11) 3. Bebouwd gebied (11)	1. Agrarisch gebied (19) 2. Bebouwd gebied (9) 3. Natuur (4)
Top 3 Water transition types	1. Flanken (24) 2. Hoge gronden (17) 3. Beekdalen (11)	1. Hoge gronden (18) 2. Stedelijk gebied/overig (10) 3. Flanken (8)	1. Hoge gronden (98) 2. Flanken (51) 3. Beekdalen (23)	1. Flanken (52) 2. Polders (18) 3. Hoge gronden (14)	1. Polders (40) 2. Hoge gronden (21) 3. Beekdalen (9)	1. Polders (20) 2. Stedelijk gebied/overig (7) 3. Uiterwaarden (6)

Table 3: Summary statistics and top 3 categories of variables per cluster

a consistent texture and high permeability. On the other hand, cluster *central_east_decr* is dominated by the STz formation (Sterksel), exhibits greater geological diversity with variations in grain size. Similarly, cluster *brabant_stat* is dominated by BXz (Boxtel), which icnludes clayey layers, indicating distinct geological characteristics again that potentially provide unique groundwater recharge dynamics within this cluster.

The water transition types that the surface level of the groundwater wells are in show further spatial hydrological distinctions among clusters. The type 'flanken', hillsides, dominates in clusters *east_decr*, *central_east_decr*, and *brabant_stat*, implying its dominance in groundwater flow and recharge, as hillsides likely serve as groundwater recharge zones. Filters from all clusters are found in the 'Hoge gronden', high grounds, but cluster *central_east_decr* is overwhelmingly dominated by filters located in these high grounds, which reflects its topological position and role as recharge area. In contrast, clusters *west_decr* and *brabant_incr* are dominantly found in 'Polders', emphasizing interactions between groundwater and surface water in low-lying areas functioning as groundwater discharge zones. 'Beekdalen', stream valley, is a considerable water transition type present within clusters *east_decr*, *central_east_decr*, and *west_decr*, which would suggest more local effects of recharge from local streams. Type 'Stedelijk gebied/overig', urban area, potentially plays an important role in the influence on groundwater filters in clusters *brabantse_wal_decr* and *brabant_incr*.

Finally, land use patterns further contextualize the behavior of the groundwater. 'Agrarisch gebied', agricultural area, dominates most clusters as the land use type a groundwater well is located at on the surface, especially clusters *east_decr*, *central_east_decr*, *brabant_stat*, *west_decr*, and *brabant_incr*, reflecting the extensive presence of agricultural activities in Noord-Brabant and the practical placement of filters on these land use types for accessibility. 'Forest' is important in clusters *east_decr*, *brabantse_wal_decr*, *central_east_decr* and *brabant_stat*; it has the highest amount of filters situated in this land-use type in cluster *central_east_decr*, where it probably plays a key role in modulating evapotranspiration. The classes of 'Infrastructure' and 'Built-up area' (Bebouwd gebied) dominate land uses in clusters *brabantse_wal_decr*, *west_decr*, and *brabant_incr*, reflecting human-induced influences on the groundwater in the immediate subsurface.

Taking these classifications together, the categorical and numerical drivers provide specific details on hydrological differences and recharge processes for each filter and its relationship to regional characteristics. The drivers provide an essential context for exploring the relationships between groundwater dynamics and environmental variables, paving the way for more detailed modelling and analysis that is described in the following section.

4.2 Unit root test

Table 4 presents the unit root test results for all variables across each cluster. The test statistic is not rejected for clusters *brabantse_wal_decr*, *west_decr* and *brabant_incr* for the variables SPI_1$_{i,t}$ and SPEI_1$_{i,t}$, which would mean that we can accept the claim that these are mean stationary I(0). For SGI$_{i,t}$, SPI_3$_{i,t}$, SPEI_3$_{i,t}$ and SPI_1$_{i,t}$ and SPEI_1$_{i,t}$ of the clusters *east_decr*, *central_east_decr* and *brabant_stat*, the test does reject the null hypothesis, so these variables contain unit roots.

Since unit root tests can have low power, especially with small sample sizes or short time series (typical conditions in environmental datasets like ours) (Breitung, 2001) and the fact that the test results vary across clusters, we include clusters *brabantse_wal_decr*, *west_decr* and *brabant_incr* in first difference unit root testing.

When taking the differences of the variables, the problem of unit roots is resolved for all variables, see table 5. The test statistic is not rejected for ΔSGI$_{i,t}$, ΔSPI_1$_{i,t}$, ΔSPEI_1$_{i,t}$, ΔSPI_3$_{i,t}$ and ΔSPEI_3$_{i,t}$, which implies that the variables are integrated of order 1, I(1).

	SGI		SPI_1		SPI_3		SPEI_1		SPEI_3	
Cluster	p-value	Reject	p-value	Reject	p-value	Reject	p-value	Reject	p-value	Reject
brabant_incr	0.00	Yes	0.75	**No**	0.00	Yes	0.72	**No**	0.00	Yes
west_decr	0.00	Yes	0.93	**No**	0.00	Yes	0.74	**No**	0.00	Yes
brabant_stat	0.00	Yes	0.00	Yes	0.00	Yes	0.03	Yes	0.00	Yes
central_east_dec	0.00	Yes	0.00	Yes	0.00	Yes	0.00	Yes	0.00	Yes
brabantse_wal_decr	0.00	Yes	0.27	**No**	0.00	Yes	0.05	**No**	0.00	Yes
east_decr	0.00	Yes	0.00	Yes	0.00	Yes	0.01	Yes	0.00	Yes
All clusters	0.00	Yes	0.00	Yes	0.00	Yes	0.00	Yes	0.00	Yes

Table 4: Results Hadri unit root test, original data

	SGI		SPI_1		SPI_3		SPEI_1		SPEI_3	
Cluster	p-value	Reject	p-value	Reject	p-value	Reject	p-value	Reject	p-value	Reject
brabant_incr	1.00	**No**	1.00	**No**	1.00	**No**	1.00	**No**	1.00	**No**
west_decr	1.00	**No**	1.00	**No**	1.00	**No**	1.00	**No**	1.00	**No**
brabant_stat	1.00	**No**	1.00	**No**	1.00	**No**	1.00	**No**	1.00	**No**
central_east_dec	1.00	**No**	1.00	**No**	1.00	**No**	1.00	**No**	1.00	**No**
brabantse_wal_decr	0.97	**No**	1.00	**No**	1.00	**No**	1.00	**No**	1.00	**No**
east_decr	0.99	**No**	1.00	**No**	1.00	**No**	1.00	**No**	1.00	**No**
All clusters	1.00	**No**	1.00	**No**	1.00	**No**	1.00	**No**	1.00	**No**

Table 5: Results Hadri unit root test, first differences

4.3 Correlation SGI - SPI & SPEI

This section examines the correlations between the SGI and the SPI and SPEI. The result show that $\Delta\text{SGI}_{i,t}$ is more strongly related to the longer-term indices than the short-term indices, such as $\Delta\text{SPI\_3}_{i,t}$ and $\Delta\text{SPEI\_3}_{i,t}$, compared to $\Delta\text{SPI\_1}_{i,t}$ and $\Delta\text{SPEI\_1}_{i,t}$. For instance, the average correlation of $\Delta\text{SGI}_{i,t}$ and $\Delta\text{SPEI\_3}_{i,t}$ is 0.394, while for $\Delta\text{SPEI\_1}_{i,t}$, it is 0.210. This suggests that the groundwater systems respond mainly to the longer, 3-months cumulative meteorological conditions rather than to the short-term, 1-month accumulation fluctuations. Also, the correlations between SPI and SPEI are very high: the mean correlation of $\Delta\text{SPI\_1}_{i,t}$ and $\Delta\text{SPEI\_1}_{i,t}$ equals 0.951, and that of $\Delta\text{SPI\_3}_{i,t}$ and $\Delta\text{SPEI\_3}_{i,t}$ equals 0.891. This implies that there is potential multicollinearity between these standardized indices. This will be formally dealt with in the first model of the pooled panel regression when looking into Variance Inflation Factors in section 4.4.

Spatially, significant variation in correlations among cluster-specific analyses was observed. In general, clusters falling within areas dominated by phreatic aquifers tend to show higher correlations, especially in the case of $\Delta\text{SGI}_{i,t}$ with $\Delta\text{SPI\_3}_{i,t}$ and $\Delta\text{SPEI\_3}_{i,t}$, given their quick response to recharge. For instance, the *brabant_stat* cluster, located in the central region with active recharge, recorded a correlation of 0.478 between $\Delta\text{SGI}_{i,t}$ and $\Delta\text{SPEI\_3}_{i,t}$. The low values obtained, for instance, reflect the delay in the response to atmospheric drivers within *brabantse_wal_decr* of confined aquifers in more western areas.

Cluster:	ΔSGI vs ΔSPI_1	ΔSGI vs ΔSPI_3	ΔSGI vs ΔSPEI_1	ΔSGI vs ΔSPEI_3	ΔSPI_1 vs ΔSPI_3	ΔSPEI_1 vs ΔSPEI_3	ΔSPI_1 vs ΔSPEI_1	ΔSPI_3 vs ΔSPEI_3
east_decr	0.043	0.191	0.047	0.265	0.437	0.442	0.934	0.878
brabantse_wal_decr	-0.001	0.179	-0.007	0.196	0.349	0.438	0.960	0.891
central_east_dec	0.109	0.306	0.101	0.394	0.423	0.444	0.954	0.867
brabant_stat	0.413	0.426	0.415	0.478	0.434	0.434	0.938	0.900
west_decr	0.258	0.405	0.268	0.430	0.405	0.416	0.967	0.924
brabant_incr	0.472	0.432	0.485	0.452	0.427	0.422	0.953	0.944
Overall	0.210	0.335	0.210	0.394	0.419	0.435	0.951	0.891

Table 6: Correlations of the difference component of different standardized variables

4.4 Multicollinearity

This section presents the VIF results, highlighting the multicollinearity between $\Delta\text{SPI\_1}_{i,t}$ and $\Delta\text{SPEI\_1}_{i,t}$ with VIF values of 9.84 and 9.85, respectively, which indicate high multicollinearity of these short-term indices. $\Delta\text{SPI\_3}_{i,t}$ and $\Delta\text{SPEI\_3}_{i,t}$ have relatively high VIFs of 4.27 and 4.38, respectively. Looking more closely to the VIFs per cluster, we saw values ranging from 3.70 to 14.10. These results are consistent with the findings of high correlations between SPI and SPEI indices, as seen in the correlation analysis in section 4.3.

The multicollinearity between these predictors will affect the use of panel regression models by causing unreliable coefficient estimates and less interpretable models. Therefore, we choose to analyze the $\Delta\text{SPI\_.}_{i,t}$ and $\Delta\text{SPEI\_.}_{i,t}$ separately in the first model of the panel regression models, in next section. For completeness, see section 4.3 for the correlation (i.e. collinearity) of the variables $\Delta\text{SPI\_1}_{i,t}$ with $\Delta\text{SPI\_3}_{i,t}$ and $\Delta\text{SPEI\_1}_{i,t}$ with $\Delta\text{SPEI\_3}_{i,t}$. By analyzing the variables separately in models 1 and 2, there will be improved model inference and it creates a more interpretable and robust framework for analyzing the SGI (Wheeler and Tiefelsdorf, 2005).

4.5 Pooled panel regression modelling

This section examines the different influences that meteorological drivers have on the SGI. Keep in mind that not all models are as representative, because they all take into account different (amounts of) drivers. Moreover, models 1 and 2 also serve as research to continue to a final model in which the influences of the most potential drivers will be found.

4.5.1 Regressing SPI and SPEI

The results from the first pooled panel regression show how $\Delta\text{SGI}_{i,t}$ is related to meteorological drivers. By comparing the SPI and SPEI models across clusters, the analysis brings out some important differences in their performance regarding explanatory power, statistical significance, and how stable the coefficients are.

The main takeaway of the first models, is that SPEI models are able to explain the SGI consistently better explain the $\Delta\text{SGI}_{i,t}$ than SPI models are. Zooming in on Model 1A (SPI without fixed effects), the R^2 values range from 0.0373 in cluster *brabantse_wal_decr* to 0.2865 in cluster *brabant_incr*. When we add fixed effects, in model 1B, the variability of $\Delta\text{SGI}_{i,t}$ explained by the SPI, drops to between 0.0004 and 0.0021. The fixed effects capture a lot of the variability that the SPI seemed to be capturing before. SPEI, on the other hand, is able to explain the $\Delta\text{SGI}_{i,t}$ time series better. In Model 1C, where SPEI without fixed effects is analyzed, the R^2 values range from 0.0776 in cluster *brabantse_wal_decr* to 0.3087 in cluster *brabant_incr*. In model 1D, where fixed effects are incorporated, the SPEI seems to perform equally to SPI when looking at the R^2 and F-statistics, as SPEI performs better in three of the six clusters. The R^2 values range from 0.0002 to 0.0042. The overall higher R^2 values together with stronger F-statistics point to evapotranspiration being an important factor in explaining fluctuations in groundwater. We will therefore further analyze ΔSGI with a focus on ΔSPEI.

ID	Cluster	β_0 (Intercept)	β_1 (ΔSPI_1)	β_2 (ΔSPI_3)	R^2	F-statistic
1	*east_decr*	-0.0071 *	-0.0082 **	0.0809 ***	0.0385	163.1407 ***
2	*brabantse_wal_decr*	0.0116 **	-0.0160 ***	0.0805 ***	0.0373	113.9510 ***
3	*central_east_decr*	0.0040	0.0007	0.1678 ***	0.0889	1480.0928 ***
4	*brabant_stat*	0.0034	0.1577 ***	0.2556 ***	0.2406	2678.6876 ***
5	*west_decr*	0.0020	0.0640 ***	0.2930 ***	0.1705	1225.3973 ***
6	*brabant_incr*	0.0065	0.2012 ***	0.2783 ***	0.2865	1272.9612 ***

*** $p < 0.01$, ** $p < 0.05$, * $p < 0.1$

Table 7: Regression results SPI, without fixed effects

ID	Cluster	β_0 (Intercept)	β_1 (ΔSPI_1)	β_2 (ΔSPI_3)	R^2	F-statistic
1	*east_decr*	-0.0072 **	-0.0149 **	0.0294 ***	0.0019	7.4668 ***
2	*brabantse_wal_decr*	0.0115 ***	-0.0306 ***	0.0181 *	0.0019	5.4810 **
3	*central_east_decr*	0.0041 *	0.0060	0.0136 ***	0.0004	5.4188 **
4	*brabant_stat*	0.0022	0.0215 ***	0.0220 ***	0.0014	11.2861 ***
5	*west_decr*	0.0013	-0.0236 ***	0.0521 ***	0.0021	12.0469 ***
6	*brabant_incr*	0.0053	0.0324 **	0.0225	0.0015	4.7577 **

*** $p < 0.01$, ** $p < 0.05$, * $p < 0.1$

Table 8: Regression results SPI, with fixed effects

ID	Cluster	β_0 (Intercept)	β_1 (ΔSPEI_1)	β_2 (ΔSPEI_3)	R^2	F-statistic
1	*east_decr*	-0.0070 *	-0.0186 ***	0.1321 ***	0.0776	342.8168 ***
2	*brabantse_wal_decr*	0.0118 **	-0.0262 ***	0.1166 ***	0.0495	153.3934 ***
3	*central_east_decr*	0.0041	-0.0268 ***	0.2746 ***	0.1617	2927.0563 ***
4	*brabant_stat*	0.0041	0.1528 ***	0.3521 ***	0.2821	3321.8006 ***
5	*west_decr*	0.0025	0.0595 ***	0.3434 ***	0.1941	1436.1401 ***
6	*brabant_incr*	0.0073	0.2155 ***	0.3062 ***	0.3087	1415.4930 ***

*** $p < 0.01$, ** $p < 0.05$, * $p < 0.1$

Table 9: Regression results SPEI, without fixed effects

ID	Cluster	β_0 (Intercept)	β_1 (ΔSPEI_1)	β_2 (ΔSPEI_3)	R^2	F-statistic
1	*east_decr*	-0.0073 **	-0.0166	0.0001	0.0004	1.4396
2	*brabantse_wal_decr*	0.0115 ***	-0.0105	-0.0075	0.0002	0.6046
3	*central_east_decr*	0.0040 *	-0.0190 ***	0.0868 ***	0.0028	42.2869 ***
4	*brabant_stat*	0.0026	0.0547 ***	0.0485 ***	0.0042	34.7942 ***
5	*west_decr*	0.0014	-0.0237 **	0.0661 ***	0.0011	6.5773 ***
6	*brabant_incr*	0.0056	0.0543 ***	0.0393	0.0023	7.1897 ***

*** $p < 0.01$, ** $p < 0.05$, * $p < 0.1$

Table 10: Regression results SPEI, with fixed effects

4.5.2 Response of groundwater by SPEI and categorical variables

Moving on to model 2, where the first lag of ΔSGI and the categorical variables are included, we see that the variance explained by the model, as measured by R^2, improves substantially, as reported in table 11 on the next page. Especially the filters within cluster *brabant_stat*, *west_decr* and *brabant_incr* can now be explained for a major part, with adjusted R^2 values of 0.34, 0.30 and 0.34, respectively. The improvements of the total variance explained in this model are mainly driven by the inclusion of the first lag of ΔSGI. The lagged value is crucial in determining what the current value of ΔSGI is in response to the standardized recharge (ΔSPEI). Remarkably, the influence of ΔSGI_{t-1} is negative across all clusters, indicating a form of reversion or lagged adjustment in groundwater systems. This can be due to natural recovery processes or temporal balancing mechanisms of an aquifer system.

Vars.	**Cluster 1:** ***east_decr***	**Cluster 2:** ***brabantse_wal_decr***	**Cluster 3:** ***central_east_decr***	**Cluster 4:** ***brabant_stat***	**Cluster 5:** ***west_decr***	**Cluster 6:** ***brabant_incr***
	Coef.	**Coef.**	**Coef.**	**Coef.**	**Coef.**	**Coef.**
Intercept	-0.0072	0.0140**	0.0108	0.0130	0.0119*	0.0167
ΔSPEI_1	-0.0369***	-0.0358***	-0.0740***	0.0319***	-0.0621***	0.1231***
ΔSPEI_3	0.1461***	0.1254***	0.3199***	0.4825***	0.4888***	0.4055***
ΔSGI_{t-1}	-0.2019***	-0.0990***	-0.2299***	-0.2865***	-0.3696***	-0.2236***
W (water trans. type)	[-0.0102, 0.0024]	[-0.0001, 0.0110]	[-0.0019, 0.0064]	[0.0021, 0.0116]	[0.0009, 0.0056]	[-0.0020, 0.0060]
AIC	6190.04	5508.61	42395.20	34233.89	22784.44	13439.45
R^2	0.1166	0.0627	0.2127	0.3399	0.2962	0.3439
Adjusted R^2	0.1159	0.0617	0.2125	0.3396	0.2958	0.3431

*** $p < 0.01$, ** $p < 0.05$, * $p < 0.1$

Table 11: Regression results of model 2 for each cluster

The water transition type is found to be the most influential categorical variable in all clusters. However, it is important to note that none of the specific types are individually statistically significant. The variables ΔSPEI_* and the lagged dependent variable ΔSGI_{t-1} do exhibit statistically significant effects.

In all clusters, the first difference of the three-month-accumulated SPEI (ΔSPEI_3) is found to have a significantly stronger influence on ΔSGI compared to the one-month-accumulated SPEI (ΔSPEI_1). Interestingly, the influence of ΔSPEI_3 is positive for all clusters, whereas coefficients of ΔSPEI_1 are negative in clusters *east_decr*, *brabantse_wal_decr*, *central_east_decr* and *west_decr*. These results highlight the importance of accounting for both the short- and short-to-medium term climatic conditions when analyzing groundwater variability in regional dimensions.

When looking at the specific coefficients of water transition types, table 13 shows, we find that the effects on ΔSGI are small, but still noteworthy:

- In clusters *east_decr*, *brabantse_wal_decr* and *brabant_incr* the water transition type 'Beekdalen' shows the highest positive influence, with coefficients of 0.0024 and 0.0110 and 0.0060 respectively. In clusters *east_decr* (-0.0102), *brabantse_wal_decr* (-0.0001) the highest negative influence is shown for the type 'Stedelijk gebied / overig' and in cluster *brabant_incr* for type 'Uiterwaarden' (-0.0020).
- Clusters *brabant_stat* and *west_decr* are only positively influenced by water transition types.
- The water transition type 'Polders' only shows positive values, which aligns with expectations, and is only included in clusters *central_east_decr*, *brabant_stat*, *west_decr* and *brabant_incr*.

The adjusted R^2 values show a significant improvement comparing to model 1, though accompanied by higher AIC values. Overall, the inclusion of the first lag and spatial variables enhances the explanatory power of Model 2. See table 13, which can be found in section 7 attached to this paper, for more detailed results on the specific coefficients for all water transition types.

4.5.3 Response of groundwater by the SPEI, its lags and the categorical and numerical variables

Finally, the first lags of ΔSPEI_* and the time-invariant numerical drivers such as elevation, proximity to extraction, proximity to KRW and big surface waters, and the filter depth are included in the regression analysis of the full model. The results of model 3A are presented in table 14 in section 7 at the end of this paper. While, the R^2 shows little improvement in model 3A compared to final model 3B, the adjusted R^2 shows slightly lower values. This confirms that the final model (3B) is the most optimal model that is analyzed in this study, and as such, only the results of this model are discussed in detail here. Summarized results of this model are shown in table 12 on page 40, with extensive results in table 15 in section 7 attached to this paper. The final model shows us that the additional variables substantially improve the explanatory power, even more so than in model 2.

We will now walk through the results of this model step by step. Concerning the influence of the ΔSPEI_*, the same results are uphold as in model 2: the ΔSPEI_3 is found to have a significantly stronger influence on ΔSGI compared to ΔSPEI_1. This pattern recurs for the lags as well in clusters *east_decr*, *brabantse_wal_decr* and *central_east_decr*. Contrastingly, in clusters *brabant_stat*, *west_decr* and *brabant_incr*, $\Delta\text{SPEI\_1}_{t-1}$ shows stronger influences than $\Delta\text{SPEI\_3}_{t-1}$. Conflicting with model 2, all coefficients of ΔSPEI_* and their lags are positive in model 3B. The coefficients of ΔSGI_{t-1}, however remain negative across all clusters, agreeing with model 2.

Next, the categorical drivers are evaluated. The water transition type remains the most influential categorical variable in all clusters except *brabant_incr*, though its coefficients are relatively small. In general, the influences are consistent with those from model 2, and the coefficients remain statistically insignificant. For cluster *brabant_incr*, land use emerges as the most influential categorical variable, where land use type 'Overig gras' has the strongest negative influence (-0.0064), and type 'Natuur' has the highest positive effect (0.0022). Note that for all land use types the coefficients are statistically insignificant as well. The specific coefficients of each water transition and land use type can be found in table 15.

Last but not least, we consider the influence of numerical drivers: elevation shows weak, statistically insignificant effects in *brabantse_wal_decr*, *central_east_decr* and *brabant_stat* of -0.0003, -0.0002 and -0.0002, respectively. Proximity to extraction locations and large surface waters provides negligible to no explanatory power across all clusters[4]. The extractions likely take place at different depths, potentially in another aquifer, thereby not directly influencing the aquifer in which the filters are positioned.

The adjusted R^2 values are considerably higher compared to model 2, with the highest values observed in *brabant_stat* (0.4860), *west_decr* (0.4307) and *brabant_incr* (0.4403), indicating strong explanatory power of the model for these clusters. In contrast, clusters *brabantse_wal_decr* (0.0909) and *east_decr* (0.1535) show the lowest adjusted R^2 values. These relatively low values are remarkable and provide us with a reason to further analyze the specific filters within these clusters in the future. Overall, the higher adjusted R^2 across most clusters shows that the final model effectively captures groundwater variability well through the analyzed variables.

In summary, model 3B is the most holistic framework for analyzing groundwater dynamics across filters included in this research. The dominant and significant drivers across all clusters are the ΔSPEI_1 and ΔSPEI_3), their lags and ΔSGI_{t-1}. In contrast, the time-invariant variables show little to no impact, where all coefficients are statistically insignificant. These results again highlight the importance of short-to-medium-term climatic conditions in explaining the variation in groundwater levels across different filters. Future research should further explore the impact of categorical and time-invariant numerical variables, possibly by analyzing a broader data panel, without focusing on small clusters. Besides, analyzing the original groundwater head values instead of the SGI values can reveal more effects and patterns.

[4]Notably, the regressed 'effects' are not covered within four decimals: 0.0000

Vars.	**Cluster 1:** ***east_decr***	**Cluster 2:** ***brabantse_wal_decr***	**Cluster 3:** ***central_east_decr***	**Cluster 4:** ***brabant_stat***	**Cluster 5:** ***west_decr***	**Cluster 6:** ***brabant_incr***
	Coef.	**Coef.**	**Coef.**	**Coef.**	**Coef.**	**Coef.**
Intercept	-0.0094	0.0161	0.0131	0.0150	0.0068	0.0168
ΔSPEI_1	0.0155***	0.0116**	0.0356***	0.2091***	0.1058***	0.2506***
ΔSPEI_3	0.1122***	0.0914***	0.2375***	0.3465***	0.3433***	0.3009***
$\Delta\text{SPEI\_1}_{t-1}$	0.0347***	0.0388***	0.1001***	0.2384***	0.2041***	0.2172***
$\Delta\text{SPEI\_3}_{t-1}$	0.0789***	0.0618***	0.1190***	0.1595***	0.1230***	0.0910***
ΔSGI_{t-1}	-0.2084***	-0.0921***	-0.2277***	-0.3735***	-0.3740***	-0.3318***
Elevation		-0.0003	-0.0002	-0.0002		0.0002
Proximity extraction	0.0000					
Proximity big SW					0.0000	0.0000
Filter depth						
W (water trans. type)	-0.0131 : 0.0022	0.0000 : 0.0085	-0.0021 : 0.0023	0.0010 : 0.0116	-0.0011 : 0.0030	
L (Land-use type)						-0.0064 : 0.0022
AIC	5841.46	5327.08	39123.07	30026.52	20266.90	12433.08
R^2	0.1544	0.0923	0.2934	0.4863	0.4312	0.4413
Adjusted R^2	0.1535	0.0909	0.2932	0.4860	0.4307	0.4403

*** $p < 0.01$, ** $p < 0.05$, * $p < 0.1$

Table 12: Regression results of final model 3B for each cluster

5 Discussion

5.1 Groundwater data limitations

The groundwater dataset used in this study presents several challenges that may have influenced the results. First, the data granularity was inconsistent: for the period before 2011 there were only one to two records per month for each filter available. Furthermore, each filter contained large periods of missing data between 2008 and 2011, which made the data before 2011 even less applicable. For post-2011 data, inconsistencies of up to 6 months were addressed with linear interpolation to create consistent daily data. A different approach of interpolation should be looked into, like model-based data with the help of the Pastas package to fill in data gaps more robustly. Extending the dataset's coverage by upsampling the data before 2011 was also considered, but implementing upsampling across all filters proved challenging. Moreover when doing so, this would create synthetic inconsistent data, while the purpose of this study was to work with raw data only. In future research, it might be useful to select filters that have continuous data for pre- and post-2011 to explore longer-term trends. In our preliminary research this came down to working only with a small amount of filters. For this reason, another possibility would be to apply model-based interpolation to cover earlier periods.

Although the original aim was to make use of hourly data, computational constraints and SQL complexities forced the use of daily records. This limited the ability to capture finer temporal dynamics of groundwater variability. Nevertheless, the daily data was sufficient for this study's scope, especially since we worked with standardized indexes that require monthly data. Future research should zoom in on making use of hourly data to analyze the variability and extremes that have now not been fully represented. This would mean not working with the monthly standardized indexes to compare filters' characteristics, but investigating fluctuations, temporal seasonalities and other influencing dynamics.

Additionally, the dataset included so called data flags for each observation, which indicate whether the observation was reliable or not, with unreliable observations for the flag values above 6. These flags were not accounted for in this analysis, which potentially introduce minor inaccuracies. Future studies should look into the definitions of the flag values and integrate flag filtering to improve the data reliability.

Last but most importantly, the time span of 12 years of data in this study is relatively short for identifying statistically robust trends. Methods like the Mann-Kendall trend test and SGI calculations (ideally) require a minimum of 30 years of data to produce reliable results (Hussain and Mahmud, 2019; Collenteur and Team, 2024). The trends reported in the results section should therefore be interpreted with care as statistical trends observed within this 12-year period, rather than long-term trends typically analyzed over a 30 year period. Similarly, the SGI calculations are affected by this short time span and should be interpreted with care, as there are only 12 values ranging between -1.769 and 1.769 per month (one value for each year). When working with at least 30 years of data, at least 30 values would be available. This limitation greatly impacts the interpretation of groundwater drought dynamics and the representativeness of the derived indices, especially the periods of drought which are determined for a minimal of 2 consecutive months having an SGI below -1.

5.2 Driver limitations

There are a few limitations to the environmental drivers that were used in this study. First of all, the precipitation and evaporation data were matched to filters based on the nearest weather station. It's worth noting that precipitation data could have been taken from nearer 'neerslag' stations of which there are many more than the weather stations. This would improve the specific location's precipitation and evaporation data, making it far more accurate and unique per filter. This can in turn influence the accuracy of standardized indices SPI and SPEI. Future research with access to more accurate precipitation and evaporation data should therefore have to decide again on the best fit between SPI or SPEI in regression model 1. Furthermore, the decision to compute the one- and three month accumulation periods for the SPI and SPEI was made, which could be reconsidered. We eventually made use of precipitation and evaporation data of at least 30 years, which made the data suitable for long-term variability and drought dynamics. Considering the relative short period of groundwater data, the decision was made to focus on the short-term groundwater dynamics and therefore also on the short-term meteorological dynamics. However, longer accumulation periods may indicate cumulative meteorological effects on the groundwater systems that could be related to long-term recharge and storage patterns. Further research based on this study could include longer accumulation periods for the SPI and SPEI or compare short- and long-term accumulation periods simultaneously to asses their impact on the dynamics of groundwater.

Secondly, the filter depths were not available for 12 out of 527 filters, which made it impossible to assign the specific geological formations to these filters. For these specific filters, the value 'Onbekend' was assigned, which slightly reduces the accuracy of geological formations as drivers in models 2 and 3. Future research should firstly complete the top and bottom depths of all filters so that their geological formation can be determined.

Another limitation lies in the use of distances to surface water bodies as predictors. The differences in the sizes of the water bodies are accounted for to a certain extent, as a distinction is made between large rivers and the smaller KRW surface water bodies. However, the real sizes of the water bodies should be taken into account in the future to see whether size (together with distance) matters in the influence of surface water to groundwater fluctuations. Furthermore, the distance to the extraction locations was calculated as overland distance. The calculation did not take into consideration the depth- or surface elevation-related differences. Moreover, only the distance to the first nearest extraction was taken into account, while all neighboring extraction locations potentially influence groundwater levels of filters. The specific years that each extraction location was active was also not inspected, which gives even more implications. Future research should therefore incorporate depth-related dynamics to refine the calculations, while also accounting for the proximity to all active neighboring extraction locations. This approach would provide a more comprehensive and accurate understanding of how groundwater interacts both with extraction locations.

Lastly, the correlations between categorical and time-invariant numerical varibles (and the SPI and SPEI) were not determined in this study. Some categorical variables are interrelated, like the land-use type and evaporation rate, and should therefore be assessed to avoid multicollinearity. Additionally, filters in certain geological formations in west Noord-

Brabant could provide insights into filters positioned in the same geological formation in eastern Noord-Brabant. However, this does not account for differences like thickness of overlying soil or the specific geological layers above individual filters. Deeper filters within the same geological formation as a shallow filter can be affected with a much longer delayed response of climatic and hydrological changes. A combined variable of filter depth and subsurface composition could be created.

5.3 Result limitations

The fact that the R^2 results in the final model are low for clusters *east_decr* and *brabantse_wal_decr* can be due to a couple of reasons. First of all making use of standardized indexes is useful for comparing dynamics of different filters. However, the way that the SGI, SPI and SPEI are set up, is a primary factor that could reduce the explained variance. We should note that the analysis focuses on the first difference of the standardized groundwater index (ΔSGI), which is a different variable on its own compared to the original groundwater levels and could further diminish explanatory power. Another potential reason for the lower R^2 values is the difference in data coverage between the groundwater and the meteorological indices. Future research should consider making use of original, non-standardized data that covers a longer period. To improve model robustness, another possibility is to work with precipitation and evaporation as individual variables without the calculation of the recharge water balance. This could increase the understanding of how each factor uniquely contributes to the dynamics of groundwater.

The inclusion of time-invariant numerical and categorical variables should be further assessed to find out whether they add significant value to regression models. While these variables provide context, their ability to explain variance of groundwater must be further assessed to be certain that their inclusion enhances the performance of the model. Future research should examine these variables in the absence of the first lags of SPEI to isolate their immediate impact on the groundwater dynamics. Also, replacing SPEI with SPI in the analysis of categorical variables may prove useful to see if simpler meteorological indices provide better explanatory power in combination with the categorical variables.

Additionally, the periodic data of water extractions in Noord-Brabant could be incorporated and could strongly enhance the explanatory power of extraction wells. The proximity to extraction wells, which is used in this study does not reflect the temporal dynamics of the withdrawal of groundwater. Future research should therefore also incorporate this data instead of distances between filters and extraction locations.

5.4 Future study directions

This study is a first attempt and introduction to how raw groundwater data of the province of Noord-Brabant can be analyzed. With this first attempt plenty of future research opportunities were identified. To start with, the cluster method used in this study, K-means, is not the most optimal and obvious method for time series clustering. That is why we recommend in the future to investigate different clustering methods that are specifically designed for temporal data. Think of dynamic time warping or feature-based clustering, which could lead to more reliable clusters being created. While this study used

six clusters, future research could also look into different cluster amounts, since two and three clusters showed higher silhouette scores.

Another option for future research could be to not work with clustering altogether. Instead, conduct a pooled regression analysis on the full SGI dataset of the 527 selected filters, and study the influences of all drivers assessed in this study in one single comprehensive regression model, rather than dividing the analysis into six different separate regression analyses. Additionally, an analysis could also be done on the entire dataset without computing standardized indexes and comparing different groundwater wells. If filters with longer periods (20-30 years or more) of data are selected, broader patterns and trends could be uncovered and general insights into groundwater dynamics provided and improved.

Finally, improving how environmental drivers are represented would boost the accuracy of groundwater modeling. Integrating better precipitation data or advancing the spatial and temporal alignment of categorical and meteorological variables could make a difference. Furthermore, also explore strategies to reduce multicollinearity between SPI and SPEI indices for more effective analysis and include these indices in models.

An identical research like this study and all the other provided potential future research options can be applied to other regions in the Netherlands as well, like the province of Limburg. If in the future a collection of similar data can be collected on a broader scale, for the whole of the Netherlands, more general insights and conclusions can be found.

6 Conclusion

Groundwater sustainability has increasingly become a subject of concern in the 21st century in regions like the province of Noord-Brabant, where climate variability, human activities, and geology interact in an increasingly threatening way to the groundwater system. This study investigated the dynamics of groundwater levels in six clusters of groundwater filters distributed across Noord-Brabant, revealing the nuanced and region-specific drivers behind fluctuations in the groundwater in a regression analysis.

6.1 Cluster specific insights

Before concluding the dynamics of each cluster, it is important to highlight that the regression analysis showed that the first differences of SPEI_1 and SPEI_3, along with their lags significantly influence SGI across all clusters. Additionally, the lag of ΔSGI is essential to determine the current ΔSGI values. Interestingly, this lag does however exhibit a strong negative influence.

- ***east_decr*:** Located in the eastern part of Noord-Brabant, this cluster exhibits the steepest decline in SGI over past 12 years. The filters in this cluster are positioned in the deepest underground layers, likely situated within confined aquifers associated with the PZWAz and Klz geological formations. The average land elevation of the filters within this cluster is the highest across all clusters, and the filters are also situated closest to extraction locations compared to other clusters. Predominant land use types are nature and agriculture, while the water transition types are mainly 'Hoge gronden' and 'Flanken'. Regression analysis identified water transition types as potential driver of the SGI, although the coefficients are statistically insignificant. However, the final model accounted only for 0.15 of the variance of in SGI, which is minimal.

- ***brabantse_wal_decr*:** This cluster is concentrated in three areas: the Brabanste Wal, the Feldbissbreuk near Tilburg and a region near Eindhoven. The filters in this cluster are located in intermediate depths of the subsurface, where the dominant geological formations are PZWAz. The land use reflects a combination of nature (Brabantse wal and Feldbissbreuk) and urbanization (area near Eindhoven), suggesting a mix of natural and anthropogenic influences on the groundwater system. This is supported by the water transition types, as 'Stedelijk gebied/overig' is dominantly present. Regression analysis indicates that elevation and water transition types provide little explanatory power for the groundwater variability in this cluster, which does align with the expectations for the Brabantse Wal and Feldbissbreuk: low lying areas where elevation and water transitions are likely to impact groundwater dynamics. The adjusted R^2 of 0.0923 emphasizes that only a small fraction of the SGI variance is explained by the model, underscoring the need for further research into the groundwater dynamics of the filters within this cluster.

- ***central_east_decr*:** This cluster is located in the central and eastern parts of Noord-Brabant, where filters are positioned at relatively elevated land levels. This is further highlighted by the dominance of 'Hoge gronden' as water transition type where most

filters are situated in. The filters are placed at an intermediate to moderately shallow depth, with considerable variability across filters within the cluster, in a geological formation that consists mainly of STz and PZWAz. The dominant land use classes in this cluster are agricultural areas and forests, underlining the interplay between natural recharge processes and human-driven influences. Regression analysis showed that elevation offers limited influence in this cluster as well. The adjusted R^2 value of 0.2932 shows that the variability in this cluster is determined for a certain part, but that there is still room for improvement. Future research has to be directed toward the additional drivers in order to capture the dynamics of SGI in this cluster better.

- ***brabant_stat*:** This cluster is spatially distributed across the entire area of Noord-Brabant, reflecting a mix of geographical and hydrological conditions. The filters are situated at locations with moderate elevations, with considerable variability in the filter depths, likely due to their widespread locations. The geological formation is predominantly BXz, which is a sandy unit generally associated with stable groundwater conditions. The dominant land use types are agricultural areas and forests. The adjusted R^2 of 0.4860 is the highest among all clusters; the analyzed drivers effectively capture groundwater variability in this cluster. However, the time-invariant numerical and categorical variables, including elevation and the water transition type, provide minimal to insignificant effects.

- ***west_decr*:** This cluster is situated in western Noord-Brabant and has elevations levels close to NAP (sea level). Filters are located in quite low depths in the subsurface, where the geological formation is primarily PZWAz. KRW surface water bodies are close and the water transition type 'Polders' is prominent, reflecting interactions between groundwater and surface water in this region. The adjusted R^2 of 0.4307 indicates that the drivers analyzed for this cluster have strong explanatory power for variability in groundwater. However, the regression coefficient of proximity to surface water is negligible, suggesting that influence of nearby surface water is not yet confirmed and could additionally by explored in the future.

- ***brabant_incr*:** This cluster is dispersed across entire Noord-Brabant. Almost all filters show a positive trend in their SGI, which is unique and is an explanation for why the time series of these filters were clustered together. The filters in this cluster are located in elevated areas close to NAP (sea level), with the lowest average elevation among all clusters. The dominant geological formation is PZWAz, reflecting sandy subsurface favorable for groundwater recharge. Land use is primarily agricultural, with high contributions from built-up areas, showing the contribution of human activities to the variation of groundwater levels. The type of water transition 'Polders' is also prevalent in this cluster, reflecting interactions with surface water systems in low-lying regions. Despite the positive trends observed, the adjusted R^2 of 0.4403 shows that while the analyzed drivers account for a considerable portion of the fluctuations of groundwater in this cluster, there remains scope for other other factors to be taken into consideration. Additional hydrogeological and anthropogenic influences should be identified to refine the understanding groundwater dynamics in

this cluster.

This study is the first attempt to explore groundwater data from Noord-Brabant, paving the way for further research. Multiple promising directions for future work have been identified. Firstly, future research should employ more sophisticated clustering approaches designed for temporal data, such as dynamic time warping and feature-based clustering. These methods potentially lead to (even) more accurate and interpretable clustered groundwater filters based on their time series characteristics. While this study focused on the analysis of six clusters, future research should explore alternative cluster amounts for more optimal and meaningful insights.

Secondly, future research could move away from clustering of groundwater filters and instead conduct a pooled regression analysis on the full SGI dataset of the 527 selected filters. This approach provides a more integrated understanding of groundwater processes by exploring all assessed drivers in one complete model, rather than separating the analysis across clusters. Moreover, future studies on modeling groundwater data could be further improved by avoiding the approach of standardizing groundwater, precipitation and evaporation data and analyze original groundwater head data directly. The broader and more general temporal feedback from raw data could uncover long-term groundwater dynamics, especially for filters that offer data of more than 20 years.

To improve modeling performance, future research should also focus on improving the representation of environmental drivers. That is, integrating better and more granular precipitation and evaporation data or refining the spatial and temporal alignment between meteorological and categorical variables. Essentially, by taking care of multicollinearity between SPI and SPEI indices, both indices can be used for analysis with greater effectiveness without compromising interpretability.

Finally, similar research approaches could be employed in alternative areas in the Netherlands, such as the province of Limburg. For more general groundwater insights, the suggested approaches should be done on a national scale. When comparable data panels from other provinces are collected and analyzed, cross-regional comparisons become possible and allow for the formulation of broader, more impactful insights regarding the groundwater sustainability of the Netherlands.

7 Acknowledgements

I would like to thank the colleagues with whom I had the pleasure to work with during my time at the Province of Noord-Brabant. Their support throughout my thesis period, and their professional experience were of great importance. Thanks to them, it was possible to get to know a big organization like the province, and also make use of the extensive database of the province. A special thanks to Maud for helping me with guiding through the first weeks of my internship, which made me feel comfortable straight away. Besides that, I want to thank Maud for the help with creating GIS maps and calculating the distances within GIS. I hope the environment that I set up in Databricks will be of great use for the province and will be continued by a fellow colleague, future intern, or student.

Next to that I would like to thank my thesis supervisors Anne van Loon, Julia Schaumberg, and Jose Henao Casas for their academic supervision and knowledge in the fields of Earth Sciences, Econometrics, and Operations Research, respectively. Their support has been crucial throughout this journey.

Figures and tables

List of Figures

List of Tables

Vars.	**Cluster 1:** ***east_decr***	**Cluster 2:** ***brabantse_wal_decr***	**Cluster 3:** ***central_east_decr***	**Cluster 4:** ***brabant_stat***	**Cluster 5:** ***west_decr***	**Cluster 6:** ***brabant_incr***
	Coef.	**Coef.**	**Coef.**	**Coef.**	**Coef.**	**Coef.**
const	-0.0072	0.0140**	0.0108	0.0130	0.0119*	0.0167
Delta_SPEI_1	-0.0369***	-0.0358***	-0.0740***	0.0319***	-0.0621***	0.1231***
Delta_SPEI_3	0.1461***	0.1254***	0.3199***	0.4825***	0.4888***	0.4055***
Lagged_SGI	-0.2019***	-0.0990***	-0.2299***	-0.2865***	-0.3696***	-0.2236***
Water_transition_type_beekdalen	0.0024	0.0110	-0.0019	0.0021	0.0015	0.0060
Water_transition_type_flanken	0.0002	0.0022	0.0001	0.0032	0.0009	-0.0004
Water_transition_type_hoge gronden	0.0004	0.0009	-0.0002	0.0031	0.0018	0.0000
Water_transition_type_polders			0.0064	0.0047	0.0021	0.0012
Water_transition_type_stedelijk gebied/overig	-0.0102	-0.0001	0.0005	0.0116	0.0056	0.0000
Water_transition_type_uiterwaarden						-0.0020
AIC	6190.04	5508.61	42395.20	34233.89	22784.44	13439.45
R^2	0.1166	0.0627	0.2127	0.3399	0.2962	0.3439
Adjusted R^2	0.1159	0.0617	0.2125	0.3396	0.2958	0.3431

*** $p < 0.01$, ** $p < 0.05$, * $p < 0.1$

Table 13: Extensive regression results of model 2 for each cluster

Vars.	**Cluster 1:** ***east_decr***	**Cluster 2:** ***brabantse_wal_decr***	**Cluster 3:** ***central_east_decr***	**Cluster 4:** ***brabant_stat***	**Cluster 5:** ***west_decr***	**Cluster 6:** ***brabant_incr***
	Coef.	**Coef.**	**Coef.**	**Coef.**	**Coef.**	**Coef.**
Intercept	-0.0168	0.0097	0.0106	0.0164	0.0113	0.0381
ΔSPEI_1	0.0155***	0.0116**	0.0357***	0.2091***	0.1058***	0.2506***
ΔSPEI_3	0.1122***	0.0914***	0.2374***	0.3465***	0.3433***	0.3010***
ΔSPEI_1$_{t-1}$	0.0347***	0.0388***	0.1003***	0.2384***	0.2041***	0.2172***
ΔSPEI_3$_{t-1}$	0.0789***	0.0618***	0.1187***	0.1595***	0.1230***	0.0910***
ΔSGI$_{t-1}$	-0.2085***	-0.0921***	-0.2283***	-0.3735***	-0.3740***	-0.3319***
W (water trans. type)	[-0.0225, 0.0040]	[-0.0017, 0.0097]	[-0.0002, 0.0023]	[-0.0015, 0.0123]	[-0.0022, 0.0056]	[-0.0260, 0.0117]
L (Land-use type)	[-0.0015, 0.0110]	[-0.0009, 0.0091]	[-0.0019, 0.0016]	[-0.0066, 0.0053]	[-0.0005, 0.0053]	[-0.0170, 0.0158]
G (Geological form.)	[-0.0093, 0.0064]	[-0.0016, 0.0057]	[-0.0076, 0.0059]	[-0.0073, 0.0085]	[-0.0126, 0.0079]	[-0.0142, 0.0189]
AIC	5872.97	5354.53	38864.07	30066.01	20312.46	12470.72
R^2	0.1545	0.0924	0.2932	0.4864	0.4312	0.4413
Adjusted R^2	0.1518	0.0888	0.2924	0.4854	0.4296	0.4387

*** $p < 0.01$, ** $p < 0.05$, * $p < 0.1$

Table 14: Regression results of model 3A including all drivers for each cluster

Vars.	**Cluster 1:** ***east_decr***	**Cluster 2:** ***brabantse_wal_decr***	**Cluster 3:** ***central_east_decr***	**Cluster 4:** ***brabant_stat***	**Cluster 5:** ***west_decr***	**Cluster 6:** ***brabant_incr***
	Coef.	**Coef.**	**Coef.**	**Coef.**	**Coef.**	**Coef.**
const	-0.0094	0.0161	0.0131	0.0150	0.0068	0.0168
Delta_SPEI_1	0.0155***	0.0116**	0.0356***	0.2091***	0.1058***	0.2506***
Delta_SPEI_3	0.1122***	0.0914***	0.2375***	0.3465***	0.3433***	0.3009***
Lagged_SPEI_1	0.0347***	0.0388***	0.1001***	0.2384***	0.2041***	0.2172***
Lagged_SPEI_3	0.0789***	0.0618***	0.1190***	0.1595***	0.1230***	0.0910***
Lagged_SGI	-0.2084***	-0.0921***	-0.2277***	-0.3735***	-0.3740***	-0.3318***
Elevation		-0.0003	-0.0002	-0.0002		
Proximity_extraction	0.0000					
Proximity_big_sw					0.0000	0.0000
Water_transition_type_beekdalen	0.0022	0.0085	-0.0021	0.0010	-0.0011	
Water_transition_type_flanken	0.0007	0.0034	-0.0009	0.0018	-0.0020	
Water_transition_type_hoge gronden	0.0009	0.0041	-0.0007	0.0020	0.0008	
Water_transition_type_polders	0.0000	0.0000***	0.0023	0.0013	0.0030	
Water_transition_type_stedelijk gebied/overig	-0.0131	0.0000	0.0009	0.0116	0.0061	
Land_use_type_Bebouwd gebied						-0.0056
Land_use_type_Infrastructuur						-0.0013
Land_use_type_Natuur						0.0022
Land_use_type_Overig gras						-0.0064
Land_use_type_Water						-0.0053
AIC	5841.46	5327.08	39123.07	30026.52	20266.90	12433.08
R^2	0.1544	0.0923	0.2934	0.4863	0.4312	0.4413
Adjusted R^2	0.1535	0.0909	0.2932	0.4860	0.4307	0.4403

*** $p < 0.01$, ** $p < 0.05$, * $p < 0.1$

Table 15: Extensive regression results of final model 3B for each cluster

References

Aghabozorgi, S., Shirkhorshidi, A. S., and Wah, T. Y. (2015). Time-series clustering–a decade review. *Information systems*, 53:16–38.

Alley, W. M., Reilly, T. E., and Franke, O. L. (2002). Sustainability of ground-water resources. *U.S. Geological Survey Circular 1186*. https://pubs.usgs.gov/circ/circ1186/.

Ascott, M. J., Bloomfield, J. P., et al. (2021). Managing groundwater supplies subject to drought: perspectives on current status and future priorities from england (uk). *Hydrogeology Journal*, 29:921–924.

Ashani, W. et al. (2022). Temperature clusters in commercial buildings using k-means and time series clustering [j]. *Energy Informatics*, 5(1):1–1.

Berthold, M. R. and Höppner, F. (2016). On clustering time series using euclidean distance and pearson correlation. *arXiv preprint arXiv:1601.02213*.

Bloomfield, J. and Marchant, B. (2013). Analysis of groundwater drought building on the standardised precipitation index approach. *Hydrology and Earth System Sciences*, 17(12):4769–4787.

Bloomfield, J. P., Marchant, B. P., and McKenzie, A. A. (2019). Changes in groundwater drought associated with anthropogenic warming. *Hydrology and Earth System Sciences*, 23(3):1393–1408.

Bourgault, P., Huard, D., Smith, T. J., Logan, T., Aoun, A., Lavoie, J., Dupuis, É., Rondeau-Genesse, G., Alegre, R., Barnes, C., et al. (2023). xclim: xarray-based climate data analytics. *Journal of Open Source Software*, 8(85):5415.

Bourgault, P., Huard, D., Smith, T. J., Logan, T., Aoun, A., Lavoie, J., Dupuis, É., Rondeau-Genesse, G., Alegre, R., Barnes, C., et al. (2024). *xclim.indices: Climate indices computation using Python*. Ouranos. Version 1.x.x.

Brakenhoff, D., Water, B., and B.V., A. (2022). Tijdreeksanalyse in de centrale slenk update 2022.

Brauns, B., Cuba, D., Bloomfield, J. P., et al. (2020a). The groundwater drought initiative (gdi): Analysing and understanding groundwater drought across europe. *Proceedings of the International Association of Hydrological Sciences*, 383:297–305.

Brauns, B., Cuba, D., Bloomfield, J. P., et al. (2020b). The groundwater drought initiative (gdi): Analysing and understanding groundwater drought across europe. *Proceedings of the International Association of Hydrological Sciences*, 383:297–305.

Breitung, J. (2001). The local power of some unit root tests for panel data. In *Nonstationary panels, panel cointegration, and dynamic panels*, pages 161–177. Emerald Group Publishing Limited.

Chow, K., O'Leary, C., Paxton-Hall, F., Lambie, D., and O'Byrne, K. (2021). Z scores, standard scores, and composite test scores explained. *Journal of Psychology and Education Research*, 29(2):7–20.

Collenteur, R. and Team, P. D. (2024). *Standardized Groundwater Index — Pastas 1.5.0 Documentation*. University of Graz, The Pastas Team. Accessed: November 25, 2024.

Cuthbert, M., Gleeson, T., Moosdorf, N., Befus, K. M., Schneider, A., Hartmann, J., and Lehner, B. (2019). Global patterns and dynamics of climate–groundwater interactions. *Nature Climate Change*, 9(2):137–141.

de Vries, L. M., Torfs, P. J. J. F., Gupta, A. K., and Stuyfzand, P. (2020). Impact of climate change on groundwater resources in the netherlands. *Water*, 12(10):2866.

Descroix, L., Nouayou, R., Kpoumié, H., and Ndomba, P. (2018). Relationships between rainfall and groundwater recharge in seasonally humid benin. *Hydrogeology Journal*, 26(7):2045–2056.

Ebeling, P., Musolff, A., Kumar, R., Hartmann, A., and Fleckenstein, J. H. (2024). Groundwater head responses to droughts across germany. *EGUsphere*, 2024:1–37.

European Environment Agency (2024). Chemical status by geological formation, wise freshwater.

Famiglietti, J. S. (2014). The global groundwater crisis. *Nature Climate Change*, 4:945–948.

Fan, X., Peterson, T. J., Henley, B. J., and Arora, M. (2023). Groundwater sensitivity to climate variations across australia. *Water Resources Research*, 59(11):e2023WR035036.

Ferguson, G. and Gleeson, T. (2012). Vulnerability of coastal aquifers to groundwater use and climate change. *Nature Climate Change*, 2:342–345.

Galloway, D. L. and Burbey, T. J. (2011). Regional land subsidence accompanying groundwater extraction. *Hydrogeology Journal*, 19(8):1459.

Geographic, N. Groundwater.

Geographic, N. (2023). Groundwater and aquifers.

Gleeson, T., Befus, K. M., Jasechko, S., Luijendijk, E., and Cardenas, M. B. (2015). The global volume and distribution of modern groundwater. *Nature Geoscience*, 9(2):161–167.

Gleeson, T., Wada, Y., Bierkens, M. F. P., and van Beek, L. P. H. (2012). Water balance of global aquifers revealed by groundwater footprint. *Nature*, 488:197–200.

Gohari, A., Eslamian, S., Mirchi, A., et al. (2023). Effects of climate change on groundwater level variations affected by human activities in the rafsanjan aquifer, iran. *Environmental Science and Pollution Research International*, 30(15):42189–42205.

Government of the Netherlands (2019). Data collecties geometrie, 2019.

Hadri, K. (2000). Testing for stationarity in heterogeneous panel data. *The Econometrics Journal*, 3(2):148–161.

Hartigan, J. A. and Wong, M. A. (1979). Algorithm as 136: A k-means clustering algorithm. *Journal of the royal statistical society. series c (applied statistics)*, 28(1):100–108.

Hiemstra, P. and Sluiter, R. (2011). Interpolation of makkink evaporation in the netherlands. Technical Report TR-327, Royal Netherlands Meteorological Institute (KNMI).

Hussain, M. and Mahmud, I. (2019). pymannkendall: a python package for non parametric mann kendall family of trend tests. *Journal of open source software*, 4(39):1556.

Hussain, M. and Mahmud, I. (2024). Pymannkendall: A python package for mann-kendall trend test. Accessed 2024-11-25.

Insights, C. S. (2020). Climate insights 2020: Drought dynamics and indicators. Online Report. Available at: https://climsystemsinsights.blob.core.windows.net/website-static-content/Climate_Insights_2020_Drought.pdf.

Ismaeel, S. S., Midi, H., and Sani, M. (2021). Robust multicollinearity diagnostic measure for fixed effect panel data model. *Malaysian Journal of Fundamental and Applied Sciences*, 17(5):636–646.

James, G., Witten, D., Hastie, T., and Tibshirani, R. (2013). *An Introduction to Statistical Learning: with Applications in R*. Springer Texts in Statistics. Springer, New York, NY, 1st edition.

Jasechko, S., Taylor, R. G., and Wada, Y. (2014). The pronounced seasonality of global groundwater recharge. *Sustainability*.

Jousma, G. and Roelofsen, F. (2004). World-wide inventory on groundwater monitoring. *Report nr. GP*, 1.

Keyantash, J. (2021). Indices for meteorological and hydrological drought. *Hydrological aspects of climate change*, pages 215–235.

Keyantash, John, N. C. f. A. R. S. E. (2023). The climate data guide: Standardized precipitation index (spi). Last modified 2023-08-19. Retrieved on 2024-11-24.

Koninklijk Nederlands Meteorologisch Instituut (KNMI) (2023). Knmi data platform.

Le Brocque, A. F., Kath, J., and Reardon-Smith, K. (2018). Chronic groundwater decline: A multi-decadal analysis of groundwater trends under extreme climate cycles. *Journal of Hydrology*, 561:976–986.

Lewandowski, H. J., Meinikmann, K., and Krause, S. (2020). *Groundwater-Surface Water Interactions*. MDPI.

Lewandowski, J., Lischeid, G., and Nützmann, G. (2009). Drivers of water level fluctuations and hydrological exchange between groundwater and surface water at the lowland river spree (germany): field study and statistical analyses. *Hydrological Processes: An International Journal*, 23(15):2117–2128.

Li, F., Feng, P., Zhang, W., and Zhang, T. (2013). An integrated groundwater management mode based on control indexes of groundwater quantity and level. *Water resources management*, 27:3273–3292.

Li, Y., Wu, G., Chen, W., Yuan, J., and Huo, M. (2024). Influence of confined water on the limit support pressure of tunnel face in weakly water-rich strata. *Journal of Central South University*, 31:2844–2859.

Marchant, B. P., Cuba, D., Brauns, B., and Bloomfield, J. P. (2022). Temporal interpolation of groundwater level hydrographs for regional drought analysis using mixed models. *Hydrogeology Journal*, 30:1801–1817.

McKee, T. B., Doesken, N. J., Kleist, J., et al. (1993). The relationship of drought frequency and duration to time scales. In *Proceedings of the 8th Conference on Applied Climatology*, volume 17, pages 179–183. Boston.

Miles, J. (2005). R-squared, adjusted r-squared. *Encyclopedia of statistics in behavioral science*.

Nationaal Georegister (2024). Metadata of dataset: Water and groundwater data in the netherlands.

Nederland, T. . D. (2024). Bro regis ii v2.2.2. Accessed: 2024-12-05.

of the Netherlands, G. (2022). Water management in the netherlands.

Owuor, S. O., Butterbach-Bahl, K., Guzha, A. C., Rufino, M. C., Pelster, D. E., Díaz-Pinés, E., and Breuer, L. (2016). Groundwater recharge rates and surface runoff response to land use and land cover changes in semi-arid environments. *Ecological Processes*, 5:1–21.

Patle, G., Singh, D., Sarangi, A., Rai, A., Khanna, M., and Sahoo, R. (2015). Time series analysis of groundwater levels and projection of future trend. *Journal of the Geological Society of India*, 85:232–242.

Paulissen, M., Nijboer, R., and Verdonschot, P. (2007). Grondwater in perspectief; een overzicht van hydrochemische watertypen in nederland. *Alterra Wageningen UR*.

Pedregosa, F., Varoquaux, G., Gramfort, A., Michel, V., Thirion, B., Grisel, O., Blondel, M., Prettenhofer, P., Weiss, R., Dubourg, V., Vanderplas, J., Passos, A., Cournapeau, D., Brucher, M., Perrot, M., and Duchesnay, E. (2011). Scikit-learn: Machine learning in Python. *Journal of Machine Learning Research*, 12:2825–2830.

Peil, N. A. (2024). History of normaal amsterdams peil. Accessed: 2024-10-22.

Pesaran, M. H. (2007). A simple panel unit root test in the presence of cross-section dependence. *Journal of applied econometrics*, 22(2):265–312.

Province of Noord Brabant (2024). Province of noord brabant official website.

Rashedy, D. A. (2024). Determining the drivers of groundwater drought in the Netherlands: a panel quantile analysis. Technical report, Vrije Universiteit Amsterdam.

Reitmeyer, M. and colleagues (2013). Hydraulic head and its role in groundwater flow and aquifer characterization. *Hydrogeology Journal*, 21(5):965–973.

Ren, X., Li, P., Wang, D., Zhang, Q., and Ning, J. (2024). Drivers and characteristics of groundwater drought under human interventions in arid and semiarid areas of china. *Journal of Hydrology*, 631:130839.

Research, W. E. (2023). Basiskaart lgn2023. CC-BY-SA License.

Rijkswaterstaat (2024). Normaal amsterdams peil (nap). Accessed: 2024-10-22.

RIVM (2018). Statutory requirements for drinking water.

Schengenga, P. and Klijn, O. (2024). Watertransitiekaart. Accessed: 2024-12-05.

Seabold, S. and Perktold, J. (2024). statsmodels: Statistical models in python. Accessed: 2024-12-16.

Sector, D. W. (2022). Future-proofing groundwater management.

Sheppard, K. (2024). linearmodels: Panel data models. Accessed: 2024-12-16.

Sutanudjaja, E., Wada, Y., and van Beek, L. (2021). Large-scale sensitivities of groundwater and surface water to groundwater withdrawal. *Hydrology and Earth System Sciences*, 25:5859–5883.

Taylor, C. J. and Alley, W. M. (2013). Circular 1217–Box A.

Taylor, R. G., Scanlon, B. R., Döll, P., Rodell, M., van Beek, R., and Wada, Y. (2013). Groundwater and climate change. *Nature Climate Change*, 3:322–329.

Team, P. D. (2024a). pandas.dataframe.corrwith. Accessed: 2024-12-05.

Team, S. D. (2024b). variance_inflation_factor. Accessed: 2024-12-05.

USGS, U. G. S. (2022). What is groundwater? https://www.usgs.gov/special-topics/water-science-school/science/groundwater.

van den Berg, H. H., Friederichs, L., Versteegh, J. F., Smeets, P. W., and de Roda Husman, A. M. (2019). How current risk assessment and risk management methods for drinking water in the netherlands cover the who water safety plan approach. *International Journal of Hygiene and Environmental Health*, 222(7):1030–1037.

van Infrastructuur en Waterstaat, M. (2024). Normaal Amsterdams Peil (NAP).

van Waterschappen, U. (2024). Grondwater - Unie van Waterschappen.

Vicente-Serrano, Sergio M, N. C. f. A. R. S. E. (2024). The climate data guide: Standardized precipitation evapotranspiration index (spei). Last modified 2024-04-22. Accessed 2024-11-25.

Vicente-Serrano, S. M., Beguería, S., and López-Moreno, J. I. (2010). A multiscalar drought index sensitive to global warming: the standardized precipitation evapotranspiration index. *Journal of climate*, 23(7):1696–1718.

Wada, Y., van Beek, L. P. H., and Bierkens, M. F. P. (2010). Modelling global water stress of the recent past: On the relative importance of trends in water demand and climate variability. *Hydrology and Earth System Sciences*, 15(7):3785–3808.

Walfish, S. (2006). A review of statistical outlier methods. *Pharmaceutical technology*, 30(11):82.

Water, U. et al. (2022). Groundwater: Making the invisible visible. *The United Nations world water development report*.

Wendt, D. E., Van Loon, A. F., Bloomfield, J. P., and Hannah, D. M. (2020). Asymmetric impact of groundwater use on groundwater droughts. *Hydrology and Earth System Sciences Discussions*, 2020:1–23.

Wheeler, D. and Tiefelsdorf, M. (2005). Multicollinearity and correlation among local regression coefficients in geographically weighted regression. *Journal of Geographical Systems*, 7(2):161–187.

Wiemann, P. and Katzfuss, M. (2023). Bayesian nonparametric generative modeling of large multivariate non-gaussian spatial fields. *Journal of Agricultural, Biological and Environmental Statistics*, 28(3):1–25.

Witte, J.-P. M., Zaadnoordijk, W. J., and Buyse, J. J. (2019). Forensic hydrology reveals why groundwater tables in the province of noord brabant (the netherlands) dropped more than expected. *Water*, 11(3):478.